Journal Pre-proof

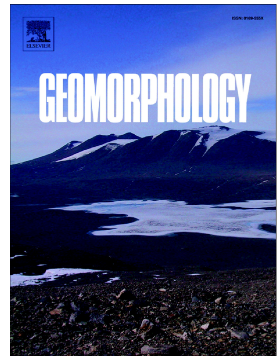

Comparing different multiple flow algorithms to calculate RUSLE factors of slope length (L) and slope steepness (S) in Switzerland

P. Bircher, H.P. Liniger, V. Prasuhn

PII: S0169-555X(19)30331-9

DOI: https://doi.org/10.1016/j.geomorph.2019.106850

Reference: GEOMOR 106850

To appear in: *Geomorphology*

Received date: 30 April 2018

Revised date: 20 August 2019

Accepted date: 21 August 2019

Please cite this article as: P. Bircher, H.P. Liniger and V. Prasuhn, Comparing different multiple flow algorithms to calculate RUSLE factors of slope length (L) and slope steepness (S) in Switzerland, *Geomorphology*(2019), https://doi.org/10.1016/j.geomorph.2019.106850

Comparing different multiple flow algorithms to calculate RUSLE factors of slope length (L) and slope steepness (S) in Switzerland

P. Bircher[1,2], H.P. Liniger[1,2], V. Prasuhn[3]

[1]Centre for Development and Environment (CDE), University of Bern, Mittelstrasse 43, 3012 Bern, Switzerland

[2]Institute of Geography, University of Bern, Hallerstrasse 12, 3012 Bern, Switzerland

[3]Agroscope, Division of Agroecology and Environment, Reckenholzstrasse 191, 8046 Zurich, Switzerland

Address: Centre for Development and Environment (CDE), University of Bern, Mittelstrasse 43, 3012 Bern, Switzerland; pascal.bircher@cde.unibe.ch

Abstract

The topographic LS-factor is one of the most difficult factors of the Revised Universal Soil Loss Equation (RUSLE) to define in a landscape with varying topography. For the application of the RUSLE not only at the plot but at catchment or landscape level, different multiple flow algorithms (MFA) have been developed and applied in various studies. However, these different MFAs in combination with various convergence values and applied at different resolutions of digital elevation models (DEM) have not been addressed so far. This publication focuses on filling this gap in the context of the agricultural area of Switzerland.

To evaluate different factors of slope steepness (S-factor) and slope length (L-factor), we tested four different multiple flow algorithms (MFA) (Deterministic Infinity (DINF), Multiple Flow Direction (MFD), Multiple Triangular Flow Direction (MTFD), Watershed (WAT)) and compared them with the MFA approach (Flow 95 in MUSLE87) used in the existing erosion risk map of Switzerland with a resolution of two metres. The MFAs we tested, used three different convergence settings and two digital terrain models (DEM) – one with a very fine two metre resolution (DEM2) and one with a coarser resolution of 25 m (DEM25) – enabling us to examine the influence of DEM resolution on the LS-factor. In total, we evaluated 21 L-factor variations to assess the significance for the prediction of the potential erosion risk. The calculations were applied at a local (test area Frienisberg, 88.7 ha) and at a regional scale (Lyss, 11,855 ha) in the agricultural Swiss Plateau. Both test areas were segmented into field blocks with an average size of 5 ha (14 field blocks in Frienisberg and 2,305 field blocks in Lyss). A field block can contain several fields with different types of agricultural land use and is delineated by surrounding hydrological barriers. For these field blocks, the various L-factors were calculated automatically using Geographic Information Systems (GIS). Finally, the LS-factors were calculated for two selected MFAs.

The L-factors calculated with the various MFAs and the high-resolution DEM2 differed negligibly in terms of statistical values (mean values, standard deviation) and in the spatial distribution of the pixels both among each other and in comparison to the L-factor of the existing erosion risk map. As expected, using the coarser DEM25 resulted in considerably lower S-factors but surprisingly in higher L-factors, so that there was little difference in the average LS values between the DEM25 and the DEM2. However, spatial distribution of the L-factor values and the soil erosion risk was much more differentiated in the DEM2 and better reflected the topography compared with the DEM25. Erosion risk hotspots such as slope depressions with concentrated runoff and thalweg erosion could be reliably identified. Moreover, the lower-resolution DEM25 was not well suited to the chosen approach with field blocks of a mean size of 5 ha, as the intersection of polygon and raster data produced edge errors depending on the clipping method. This study showed that a high-resolution DEM was more important for the calculation of the LS-factor and potential soil erosion risk than the choice of MFA, and that the calculation of LS-factors based on field blocks offered a number of advantages mainly in determining the channel network and maximum flow length .

Key words: Soil erosion, RUSLE, LS-factor, Multiple Flow Algorithm, DEM, GIS

1. Introduction:

Soil degradation including soil erosion is a well-known global, regional, and local problem highlighted by several stakeholders such as the Food and Agriculture Organization (FAO), farmers, policymakers, and social and natural scientists (Keizer et al. 2016; Borrelli et al. 2017). Soil loss is an important topic and was discussed at many conferences during the United Nations-declared International Year of Soils 2015. It was also a topic of numerous meetings of the United Nations Development Programme (UNDP 2015) in the run-up to establishment of the UN Sustainable Development Goals.

Water erosion is often modelled for short-term periods, with physical-event-based models in small or only a few catchments (Morgan 2009; Mitasova et al. 2013). On the other hand numerous semi-empirical, plot-field-scale models exist for assessing soil erosion risk at regional, national, continental and world-wide scales (Panagos et al. 2015b; Borrelli et al. 2017; Benavidez et al. 2018). Calculating a nationwide long-term erosion risk map requires large quantities of data that are not available from the official authorities in wished quality. An empirical-based model like the Universal Soil Loss Equation (USLE) (Wischmeier and Smith 1978) and revised versions such as the Revised Universal Soil Loss Equation (RUSLE) (Renard et al. 1997), allow the use of data of varying accuracy. Therefore, the USLE and RUSLE are still the most frequently used erosion models despite numerous deficiencies, weaknesses, and limits (Favis-Mortlock et al. 2001; Boardman 2006; Benavidez et al. 2018). The combination of geographical information systems (GIS) and computer processing power allows better resolution input data to be used for modelling studies and projects. Consequently, many RUSLE-based erosion risk models were recently established in several countries with databases of various resolutions (e.g. Borrelli et al. 2016, Italy, 25 m; Kotremba et al. 2016, Rheinland-Pfalz in Germany, 1 m; Hrabalíková and Janeček 2017, Czech Republic, 5 m), as well for the entire European area (Panagos et al. 2015b, 25 m) and at a global scale (Naipal et al. 2015; Borrelli et al. 2017, 250 m). Often, the RUSLE approach is combined with remote sensing data to calculate the RUSLE-factors (Ismail and Ravichandran 2008; Kamaludin et al. 2013) or with sediment delivery models for sediment yield (Fernandez et al. 2003; Fu et al. 2006; Bhattarai and Dutta 2007).

Next to the C-factor, the LS-factor is the most sensitive parameter in estimating soil loss in RUSLE (Auerswald 1987; Panagos et al. 2015a). The L and S factors are combined as the topographic LS-factor. The slope length factor (L) is more problematic to calculate than the slope steepness factor (S) and it plays a key role for the application of the RUSLE erosion model (Hickey 2000; Winchell et al. 2008; Hoffmann et al. 2013; Oliveira et al. 2013; Liu et al. 2015; Hrabalíková and Janeček 2017). For catchment-scale studies the one-dimensional slope length factor of individual slopes in the USLE was replaced by the upslope contributing area in newer studies to respect the topography of complex watersheds or big two- or three-dimensional areas. Different approaches and algorithms to calculate these slope length factors was described by Van Remortel et al. (2001), Garcia Rodriguez and Gimenez Suarez (2010), Hoffmann et al. 2013, Oliveira et al. (2013), and Zhang et al. (2017). These are the unit stream power method (Moore and Burch 1986; Moore et al. 1991; Mitasova et al. 1996), raster grid cumulation (Hickey 2000), and upslope contributing area methods (Moore and Wilson 1992, Desmet and Govers 1996). The method of Desmet und Govers (1996) was recently improved by several authors: Winchell et al. (2008) as well as Garcia Rodriguez and Gimenez Suarez (2012). Panagos et al. (2015a) used the unit contributing area approach based on Desmet and Govers (1996) to calculate LS-factors for Europe, and Borrelli et al. (2017) calculated it for the whole world. To avoid possible overestimation and extreme values of L-factors, often theoretical maximum values are defined. Those maximum values are often 122 m or the equivalent length in number of pixels depending on resolution because surface runoff will usually concentrate in less than 122 m, although longer slope-lengths are occasionally found (Fu et al. 2006; Yang 2015; Borrelli et al. 2017). In other studies, thresholds for slope changes that indicate deposition were used (Liu et al. 2011; Zhang et al. 2013; Yang 2015; Zhang et al. 2017). Based on the two approaches of Hickey (2000) and Van Remortel et al. (2001), new models and tools for LS-factor calculations were developed by Liu et al. (2011), Zhang et al. (2013), Yang (2015), and Zhang et al. (2017), including deposition zones, channel networks, and convergence flow areas with cut-off effects or turning points.

The upslope contributing area, also known as flow accumulation, contains the total upslope area or all upslope pixels flowing in single pixels. The choice of a flow-routing algorithm has a big influence on the calculation of the contributing area (Wilson et al. 2008). Multiple flow direction algorithms are better accepted than single flow algorithms, because convergent and divergent flows are better represented in real landscapes (Wilson et al. 2008; Orlandini et al. 2012). Some multiple flow direction algorithms can describe overland flow dispersion (Freeman 1991; Quinn et al. 1991; Tarboton 1997; Seibert and McGlynn 2007). These algorithms are not only used for LS-factor determination in soil erosion modelling, but are also important for identifying critical source areas in hydrological modelling (Thomas et al. 2016; Thomas et al. 2017). Even though there have been significant advances in recent decades in erosion modelling with RUSLE, especially thanks to geospatial technologies such as GIS (Benavidez et al. 2018; Borrelli et al. 2018), there are hardly any comparative studies on different available LS-factor calculations and their variations. Accordingly, little is known about whether and why they differ and how big the differences are.

To ensure hydrological connectivity DEM correction is an important aspect of hydrological modelling and soil erosion modelling. The correction or filling of the DEM provides hydrological connectivity and also corrects artefacts of DEM production. In advance of the LS-factor calculation and the use of a high-resolution DEM with multiple flow algorithms, most newer studies pre-process the DEM, applying DEM correction (Van Remortel et al. 2001; Liu et al. 2015; Yang 2015). In hydrological modelling, a total connectivity without absolute sinks is necessary to model the flow pathways to the outlet of the catchment area (Thomas et al. 2017). The necessity of DEM correction also depends on the accuracy and resolution of the DEM. Lane et al. (2004) distinguish between pits, hollows, and flats. Pits are mostly single cells with minimal slope to neighbouring cells, and often they are artefacts or errors of the DEM. Hollows are multiple neighbouring pixels creating drainless sinks. Flats are planar areas without flow direction. The problem is how to distinguish between real sinks and artificial sinks (artefacts of the DEM) to best represent reality (Lane et al. 2004; Thomas et al. 2016). Different methods have been developed to fill flow sinks (Planchon and Darboux 2002; Wang and Liu

2006). To date, there are hardly any comparative studies and reliable statements about the benefits or problems of different DEM correction methods for LS-factor calculation.

Several authors have mentioned the fundamental importance for soil erosion risk assessment of cell size and the accuracy of DEMs on the production of different terrain parameters like slope steepness and slope length (Hickey 2000; Thompson et al. 2001; Kienzle 2004). Local artefacts can occur when the resolution is very high or the accuracy is low (Hengl 2006). It is accepted that, the lower the resolution of a DEM, the greater the smoothing effects that reduce the slope steepness (Kienzle 2004). For example, in a comparison of DEMs with 5, 10, 25, 50, and 100 m raster cell sizes, Kienzle (2004) determined an underestimation of slope steepness with bigger raster cell data, concluding that raster cell sizes > 25 m are no longer able to accurately represent steep slopes. On the other hand, a very high-resolution DEM can lead to very high LS-factor values and therefore to an overestimation of soil erosion risk by RUSLE. Many studies show an overestimation of the risk of erosion based on the RUSLE approach compared to measured soil erosion (Abu Hammad et al. 2004, Rymszewicz et al. 2015). Some researchers have tried to understand the resolution effect of the digital elevation models (DEM) on the RUSLE topographic LS-factor, but most of them use a DEM resolution of 10 m or coarser: e.g. Claessens et al. (2005) [10–100 m], Wu et al. (2005) [10m–250m], and Mondal et al. (2017) [30–330 m]. Higher-resolution DEMs were only used by Deumlich (2012) [1–25 m], Fu et al. (2015) [2–30 m], Yang (2015) [5–100m], and Wang et al. (2016) [2–30m]. So far, it has not yet been systematically examined whether different DEM resolutions result in different LS-factor values and whether use of high-resolution DEMs results in higher L-, S-, and LS-factors.

Switzerland already has an online high-resolution [2 m] erosion risk map (ERM2) for agricultural land, hosted by the government (Prasuhn et al. 2013). The ERM2 is based on the MUSLE 87 approach (Moore and Burch 1986; Moore et al. 1991) and was calculated in ArcView on a 2 m grid with an outdated plugin which is no longer supported (AVErosion, Vers 1.1, Schäuble 2005). The MUSLE 87 approach involves the possibility of long-term erosion risk calculations with the program Flow 95, a multiple flow algorithm (MFA) like the Desmet and Govers (1996) approach. The ERM2 has proved its worth in practice as an aid to the enforcement of legal bases and as a consulting tool for farmers and agricultural advisors (Prasuhn et al. 2013). However, it needs to be upgraded, as it is based on data older than 2010 and only up-to-date maps of all RUSLE input parameters and the calculated erosion risk are credible to farmers and public authorities. The DEM of the ERM2 was created with LIDAR in 2007 and was the first version of a DEM with a 2 m resolution covering all of Switzerland up to 2,000 m altitude. This first version of the DEM contains artefacts because of production errors, like cutting effects between different national map extents, and technical errors (Swisstopo 2009). It is therefore essential to find an adequate replacement for the existing approach. In addition to using the latest data, it is very important to recalculate the LS-factor – the most important factor in the potential risk of erosion. The current ERM2 has led to high soil erosion risk values compared to measured soil erosion (Prasuhn 2011). We suspected one of the reasons for this to be that the DEM's high resolution of 2 m leads to high LS-factor values. In our study we therefore also examine different DEM resolutions, using a 2 m DEM (DEM2) and a 25 m DEM (DEM25). For computational reasons, the 21 different L-factor calculation methods cannot be tested for the whole agricultural area of Switzerland (7,686,981 ha or 19,217 million pixels including grassland and alpine area). In this study, we therefore analysed two test areas with different map scales.

Overall, the current state of the art can be summarized by stating that DEM data are available almost everywhere in the world – but differ in quality and spatial resolution. These data can easily be prepared using GIS technologies, and standard software packages offer a variety of ways to then calculate S-, L-, and LS-factors.

In this article, we present an extensive comparative analysis with which we pursued two aims. The first was to show whether different multiple flow algorithms (MFAs) and convergence options result in different modelled water flow properties influencing LS-factor calculations. To find this out, we compared four common MFAs (Deterministic Infinity (DINF), Multiple Flow Direction (MFD), Multiple Triangular Flow Direction (MTFD), Watershed (WAT)) for L-factor calculation, including varying convergence values among each other and with the MFA of the current ERM2 (Flow 95 from

MUSLE87). The second aim was to examine the effect of two DEMs with different resolutions (2 m vs 25 m). We expected the use of a very high-resolution DEM (2m) to result in higher S-, L-, and LS-factor values and therefore in a higher potential erosion risk. All in all, we analysed 21 variations at a local (Frienisberg) and a regional (Lyss) scale, in areas typical of the Swiss Plateau. The calculations for both test areas are processed in field blocks or micro-catchments of 5 ha mean size. These field blocks enabled us to distinguish between agricultural and non-agricultural areas and to adequately represent the topographic complexity and patchiness of landscapes in Switzerland. The LS-factor calculations were then executed with two chosen MFAs and both DEMs. Our results are intended to contribute to a better understanding of different L- and LS-factor calculations and to provide a basis for informed selection of suitable calculation methods so as to model soil erosion risk as realistically as possible using RUSLE.

2. Methods:

2.1. Methodological overview

This section provides a brief guide to the huge amount of data and results produced in this study. We processed 20 L-factor calculations with three convergence options plus the MUSLE 87 approach used in the current ERM2. This was done for two different test areas, which we explain in detail in section 2.2 below. Further, we used two different DEMs and two different clipping approaches (hard and soft) (Table 1). Finally, we compared the resulting L-, S- and LS-factors. More details about the methods are provided in sections 2.2 and 2.3.

Table 1: Overview of the 21 approaches and basic data (in bold frame) used for comparison of statistical features; Lyss and Frienisberg are the two test areas (see section 2.2)

Tool	Algorithm	Convergence value	Resolution of DEM		Test area		Clipping		L-factor[1]	S-factor[2]	LS-factor[3]
			2 m	25	Lyss	Frienisberg	soft	hard			
Saga Gis	**MFD**	0	x	x	x	x	x		x	x	
		1.1	x	x	x	x	x	x	x	x	x
		1.25	x	x	x	x	x		x	x	
	MTFD	0	x	x	x	x	x		x	x	
		1.1	x	x	x	x	x		x	x	
		1.25	x	x	x	x	x		x	x	
GrassGis	**WAT**	1	x	x	x	x	x		x	x	
		5	x	x	x	x	x	x	x	x	x
		10	x	x	x	x	x		x	x	
Saga Gis	**DINF**	1.1	x	x	x	x	x		x	x	
AVErosion in ArcView	**MUSLE 87**	-	x		x	x	x		x		

[1] Calculated according to Desmet & Govers 1996
[2] Calculated according to McCool 1987
[3] Product of 1 and 2

MFD: Freeman 1991; MTFD: Seibert and McGlynn 2007; WAT: Ehlschlaeger 1989, Quinn et al. 1991; DINF: Tarboton 1997; MUSLE 87: Moore and Burch 1986, Moore et al. 1991

2.2. Study area

The Frienisberg test area represents the local scale, comprising 88.7 ha or 221,673 pixels at 2 x 2 m. Frienisberg has a varied topography and is a hilly region between the northern Prealps and the Jurassic alps on the Swiss Plateau (Figure 1). It is located about 20 km north-west of Bern, with altitudes ranging from 591 to 729 m (Table 2). The topography consists of very steep (slopes > 24.2°) and flat areas (slopes < 2.9°), with ridges, channels, peaks, and very small pits (sinks). Most soils in the test area are quite permeable Cambisols and Luvisols over ground moraine; they are mostly sandy loams which have been rated as having moderate erodibility. The predominant family farms apply mixed farming methods of growing crops and keeping livestock. Crop rotations are versatile and mostly have a high proportion of temporary grass-clover mixtures. The Frienisberg area lies in the moderate climate zone with an annual average temperature of approximately 8.5 °C and annual precipitation from 1035 to 1150 mm. Frienisberg is one of five long-term monitoring areas in which erosion damage has been mapped since 1987. Over a period of 10 years, the visible erosion features on 203 arable fields in the area were continuously mapped and quantified by Prasuhn (2011; 2012). Although the average soil loss was relatively low (0.75 t ha^{-1} yr^{-1}), the maximal annual erosion in a single field was 96 t. Rill and ephemeral gully erosion accounted for 75%, while inter-rill erosion took place only in 25% of the cases (Prasuhn 2011). Gully erosion has not been reported so far. Frienisberg is also one of 17 case studies around Europe in an EU project called RECARE (Preventing and Remediating Degradation of Soils in Europe through Land Care, 2013–2018, www.recare-project.eu), which investigated the influence of measures to combat different soil threats. Frienisberg is part of the Lyss test area. This second, larger national map extent (1:25,000) represented the regional scale in our study, covering 11,855 ha or 29,637,170 pixels of 2 x 2 m. The Lyss area consists mainly of arable land typical of the Swiss Plateau. Topographically it is more balanced than the Frienisberg area, with fewer steep and more flat slopes, as well as a few small plains. The L-factor calculation and its statistical evaluation are mainly based on the local scale (Frienisberg) (Figure 1c); the DEM correction, slope calculation, as well as S-factor and LS-factor calculations focus on the bigger map extent of Lyss (Figure 1b).

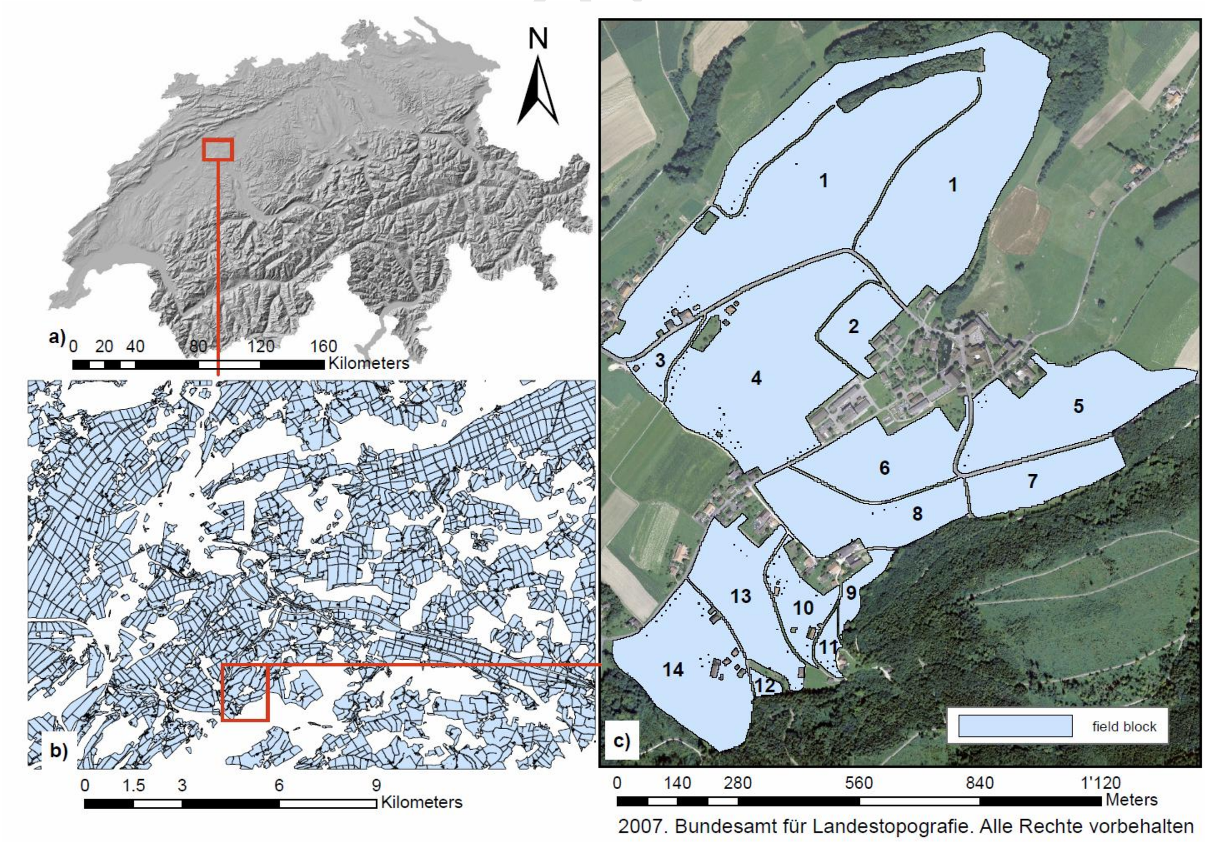

Figure 1: Overview of study area; a) Map of Switzerland, b) 2,305 field blocks of Lyss national map extent at 1:25,000, c) extent of Frienisberg with numbered field blocks (SwissALTI3D 2015, Vector 25 2008, Swisstopo 2008)

2.3. Basic data and calculations

2.3.1. Digital elevation model (DEM)

We used two different DEMs available for the whole area of Switzerland to study the influence of raster size and accuracy of the data. The DEM2 we used was produced with Light Detection and Ranging (LIDAR) technology. Vertical accuracy, at ± 0.5 m 1 σ, is very high (Swisstopo 2015). The DEM25 was derived from the 1:25,000 map set of Switzerland. Mean deviation is 1.5 m in the Jura region and Swiss Plateau, 2 m in the Prealps and Ticino, and 3–8 m in the Alps (Swisstopo 2005). The differences in mean value of the two DEMs in metres above sea level for both test areas (Frienisberg and Lyss) are very low (Table 2).

Table 2: Comparison of statistic features of the 2 m and the 25 m DEM based on the 25 m mask for Frienisberg and Lyss; [m a. s. l. = meters above sea level]; mask (see Table 4)

	Frienisberg, masked		Lyss, masked	
Resolution of DEM	2 m	25 m	2 m	25 m
Number of cells (N)	151,280	941	20,745,979	132,829
Area [ha]	60.5	58.8	8,298	8,302
Minimum [m a. s. l.]	591	600.5	431.6	432.1
Maximum [m a. s. l.]	728	722.7	789.5	789.8
Mean [m a. s. l.]	660.8	660.7	521.3	521.5
Standard deviation [m a. s. l.]	26.8	26.6	69.9	69.8

2.3.2. Digital elevation model (DEM) correction

Using a raw DEM generated with LIDAR results in a number of hydrological sinks and artefacts acting as absolute sinks. These absolute sinks can be avoided using a fill function, to obtain a connected DEM essential for hydrological models. This correction of the DEM is an important step to hydrologically connect the DEM and was done with the Arc Hydro Tools in ArcGis v.10.2.2, reported in Maidment (2002). Different fill heights lead to a more or less flooded area or a more or less hydrologically connected DEM. Therefore, different fill heights were tested (0.2; 0.5; 2.0; 4.0; 6.0 m; fill all) to see how big the affected area is. Fill All corresponds to a DEM completely hydrologically connected. During the application of DEM correction, a minimum slope gradient between neighbouring cells of 0.1° was enforced. This DEM correction was applied in a pre-processing to both the DEM2 and the DEM25 (Maidment 2002). Afterwards, the slope (Zevenbergen and Thorne 1987) and catchment area are calculated in Saga-Gis and GrassGis, and the results are included in the S-factor and L-factor calculation.

2.3.3. Field block map

The Swiss landscape is characterized by topographic complexity, patchiness, and small-scale farming (Alder et al. 2015). This makes field blocks – a reference unit used in Germany (Volk et al., 2010; Tetzlaff et al., 2013) – a good basis for calculating the L-factor. The landscape model (Vector 25) as basis data for the field block map in the ERM2 is also derived from Swisstopo (2008). Field blocks were extracted with the same approach mentioned in Prasuhn et al. (2013). The agricultural area of Switzerland is represented in the field blocks and covers grassland, meadows, pastures, crop fields, and grapes. Field blocks were delineated by surrounding hydrological barriers like roads, railways, forests, villages, rivers, lakes, and other objects that prevent a continuous water flow. A field block can thus contain several cultivation plots, feature different types of use (arable land, permanent grassland, vineyards, or different field crops), and be cultivated by different farmers. These field blocks serve as the calculation unit for the different LS-factor methods and represent hydrological micro-catchments, into which no water can flow from the outside and no water can leave. For each grid cell in a field block we calculated the L-, S-, and LS-factors. Frienisberg consists of 14 field blocks with a mean size of 6.3 ha; Lyss consists of 2,305 field blocks with a mean size of 5.1 ha (Figure 1). The field block map of Switzerland includes 180,920 field blocks ranging from 0.25 ha to 1,444 ha in size, with a mean value of 5.0 ha, a standard deviation of 11.0 ha, and a median of 2.4 ha (Prasuhn et al. 2013).

2.3.4. Clipping method

A further factor influencing the waterflow calculation is the clipping method between vector (field block) and raster data with different resolutions (DEM2 vs DEM25). Using a soft clipping method in GIS systems means that the accuracy of the DEM used and its raster cells are more important than the accuracy of the cutting elements (field blocks, vector data). By contrast, with the hard clipping method, the accuracy of the vector data (field blocks) is more important than the raster cells of the

DEM. For example, when soft clipping is applied with the DEM25, small roads are ignored to preserve information. But when hard clipping is applied, all small roads are cut into the DEM, regardless of data loss (Table 4, Figure 8). The hard clipping method also provides a suitable mask based on the DEM25 for statistical analyses. For the statistical comparison of the S, L, and LS-factor values of the 2 m and 25 m elevation models, the 2 m model was always scaled down to the size of the 25 m model (masked, hard clipped). This results in considerable data loss towards the boundary of the field blocks on both DEMs due to the edge effects on the 25 m model. However, to calculate LS-factors for the whole of Switzerland with the DEM2, we used the soft clipping method without masking. With the DEM2, the clipping method is not important and the data loss is very low. In this article, the soft clipping method without masking was also used in all maps with DEM2.

2.3.5. USLE approaches and derivates

The RUSLE/MUSLE 87 (Eq.1) approach is based on the widely used USLE estimation (Wischmeier and Smith 1978), and consists of six factors, where L is the slope length factor [no unit], S is the slope steepness factor [no unit], K is soil erodibility factor [$t*ha*h*ha^{-1}*MJ^{-1}*mm^{-1}$], R is the rainfall and run-off erosivity factor [$MJ*mm*ha^{-1}*h^{-1}*y^{-1}$], C [no unit] is the cover and management factor, and P [no unit] is the support practice factor. The multiplication of the factors L * S * K * R results in the potential erosion risk for each grid cell, whereas the multiplication of all six factors leads to the actual soil erosion risk in tonnes per hectare and year (Wischmeier and Smith 1978, Renard et al. 1997). The calculation in this study is limited to the potential soil erosion risk. The computations are based on a regular grid of equal-sized grid cells (2 m x 2 m or 25 m x 25 m).

$$A = L * S * K * R * C * P \qquad \text{Eq. 1}$$

The USLE/RUSLE approach was originally designed to predict long-term average annual soil loss associated with rill and inter-rill erosion on hillslopes, but not gully erosion or deposition of soil material. Furthermore the RUSLE-approach base on a standard plot with 22.1 m length and a slope of 5.1°. The use of multiple flow algorithms makes it possible to distribute virtual water on various deeper neighbouring cells, which leads to results that better reflect erosive processes on a complex topography. In addition, ephemeral gully erosion (thalweg erosion) is represented well (Prasuhn 2011). Finally, the USLE/RUSLE approach only predicts "edge-of-field" erosion, while catchment erosion estimates are adjusted downward by a sediment delivery ratio (Boomer et al. 2008).

2.3.6. L- and S-factor approaches and combinations

There are numerous LS-factor calculation methods (Wischmeier and Smith 1978; Moore and Burch 1986; Moore et al. 1991; Renard et al. 1997; Böhner and Selige 2006) with connected and separated L- and S-factor calculations. Connected LS-factor calculations (Moore and Burch 1986; Moore et al. 1991; Böhner and Selige 2006) use a smoothing calculation, like mean slope values for the catchment calculation or constant values for rill and inter-rill properties (Moore and Burch 1986; Moore et al. 1991; Moore and Wilson 1992). To consider the precise topography given by a high-resolution 2 m-DEM and also for confirmability, we applied separate S- and L-factor calculations.

2.3.7. S-factor calculation

Many S-factor equations exist in the literature, valid and measured for inclinations of up to 9.1°–11.3° (Zingg 1940; Smith and Whitt 1947; Smith and Wischmeier 1957; Wischmeier and Smith 1978; McCool et al. 1987; Nearing 1997). Other studies extrapolated or assessed the S-factor to steeper inclinations like 28.8° (Hurni 1979; Liu et al. 1994). To select a suitable method for our area, we tested different approaches based on virtual slope values (slopes 0°–45°) (Figure 2). There are different properties of slope and S-factor relations among the chosen equations, especially at high slopes > 10 degrees. Most arable land in Switzerland is on slopes < 10 degrees (see section 3.2), where the differences of the compared approaches are not very high. Therefore, we opted for the approach of Renard et al. (1997), which is used in the RUSLE and based on Mc Cool et al. (1987). This approach was also used by Prasuhn et al. (2013) for the current erosion risk map of Switzerland.

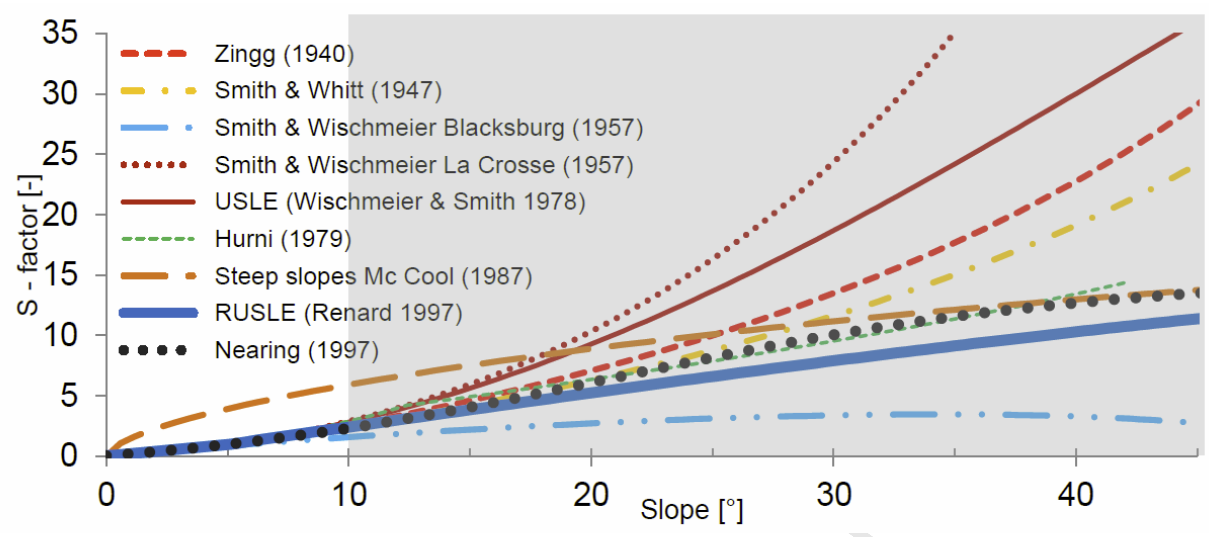

Figure 2: Selection of different S-factor approaches calculated for a virtual slope steepness of 45° separated into steep slopes > 10° and low slopes < 10°

Slope was computed in SAGA-Gis (System for Automated Geoscientific Analyses) from the corrected DEM using the Zevenbergen and Thorne (1987) method for both DEMs. The S-factor (Eq.2 and Eq.3) was calculated with the well-known RUSLE approach in Renard et al. (1997) based on McCool et al. (1987), where S_{low} is for slopes smaller than 5.1° and S_{steep} is for slopes equal or greater than 5.1°. θ is the slope in degrees.

$$S_{low} = 10.8 * \sin(\theta) + 0.03 \; for \; \theta < 5.1° \qquad \text{Eq. 2}$$

$$S_{steep} = 16.8 * \sin(\theta) - 0.5 \; for \; \theta \geq 5.1° \qquad \text{Eq. 3}$$

2.3.8. L-factor calculation

The L-factor (Eq.4) was calculated with the approach of Desmet und Govers (1996), where A is the upslope contributing area in square metres, d is the raster resolution in metres, m (Eq.5) is the slope length exponent showing the relation between rill and inter-rill erosion, β (Eq.6) is the slope direction, and θ is the slope angle in degrees.

$$L_{factor} = \frac{(A+d^2)^{m+1} - A^{m+1}}{d^{m+2} * 22.13^m} \qquad \text{Eq. 4}$$

$$m = \frac{\beta}{1+\beta} \qquad \text{Eq. 5}$$

$$\beta = \left(\frac{sin(\theta)}{0.0896}\right) / (3 * sin(\theta)^{0.8} + 0.56) \qquad \text{Eq. 6}$$

The L-factor approach was combined with four different multiple flow direction algorithms and compared with the approach of Schäuble (2005) from the current ERM2, referred to as MUSLE 87:

- Deterministic Infinity (DINF), SagaGis
- Multiple Flow Direction (MFD), SagaGis
- Multiple Triangular Flow Direction (MTFD), SagaGis
- Watershed (WAT), GrassGis
- MUSLE 87, AVErosion in ArcView

The DINF algorithm provides pseudo multiple flow properties because it only respects the next two deeper cells of a raster file (Tarboton 1997). The MFD (Freeman 1991) algorithm shares virtual water with every next deeper raster cell and the MTFD combines the DINF properties and the MFD properties and concentrates water flow in valleys, depressions, and natural sinks (Seibert and McGlynn 2007). The WAT approach computes the water flow like an MFA and includes an option with least-cost search in the algorithm (Ehlschlaeger 1989; Quinn et al. 1991). Other MFAs like Terraflow (Arge et al. 2003) in GrassGis, Rho (Fairfield and Leymarie 1991), and DEMON (Costa-Cabral and Burges 1994) algorithms in Saga-Gis were not processed due to calculation problems and the need for some physical parameters, such as amount or content of water and soil properties for event-based models.

2.3.9. LS-factor

L-and S-factors can be combined through multiplication and lead to different values depending on approaches and resolutions. Some LS-factor calculations are coupled to simplify the process of modelling in programmes like SagaGis or GrassGis but can hinder the confirmability (Moore et al. 1991; Moore and Wilson 1992; Böhner and Selige 2006). Most of the available LS algorithms are already implemented within GIS software, such as IDRISI, SagaGIS, GrassGis, ArcGIS, etc. SagaGis v.2.1.2 and GrassGis v.7.0.3 use different options to respect convergence properties of water flow. In SagaGis the default value is 1.1, the minimum value is 0, and the maximum is 1.25. In GrassGis the default value is 5, the minimum value is 1, and the maximum value is 10. These options were tested in each case. For both tools SagaGis and GrassGis, low convergence (0, 1) values allow the virtual water flows with higher dispersion and for high convergence values (1.25, 10) the water flows in a more concentrated manner.

3. Results

3.1. Hydrological connectivity

Considering different filling heights for a DEM correction allows the elimination of artefacts and small sinks of varying sizes. Depending on the fill height, more or less pixels/area are filled or flooded and hydrologically connected (Table 3) in Lyss. "Fill All" means a completely hydrologically connected DEM, where big sinks (e.g. depressions) are filled. Fill heights of 0.2, 0.5, 2.0, and 4.0 m lead to very similar results with only about 4% of filled area in Lyss. With about 14% of filled or flooded area in Lyss, fill heights higher than 4 m have considerably more influence (Table 3). To consider only a partly filled DEM – respecting bigger sinks as not connected – the fill height 0.5 m was applied on both DEMs and used for all following calculations.

Table 3: Different fill heights and filled agricultural area in hectares and in % for Lyss [11,854.9 ha] and DEM2.

Fill height [m]	**0.2**	**0.5**	**2.0**	**4.0**	**6.0**	**Fill All**
Filled area [ha]	426.1	427.5	428.4	428.6	1705.3	1705.8
Filled area [%]	3.59	3.60	3.61	3.62	14.38	14.39

The clipping effect of the 25 m grid with the field block map shows big differences in the number of raster cells and the area size between the soft clipping and the hard clipping method respectively, independent of region (Table 4). Using the DEM25 with the hard clipping method, 33% (Lyss) or 31% (Frienisberg) fewer pixels/less area is captured compared to the soft clipping method. Similar values of area loss resulted when soft vs hard clipping (masked) method is compared regarding the DEM2. In contrast, the area of the field block polygons and soft clipped raster cells corresponded very well to the DEM2. For the DEM25, the deviations are slightly larger, but still small (Table 4). This effect also influences slope and S-factor calculations (see section 3.2).

Table 4: Differences of soft and hard [mask] clipping methods for statistical analysis and comparison with DEM2, DEM25 and original polygon data; n = number of raster cells or polygons

Test area		**Frienisberg**		**Lyss**
Clipping method [resolution]	**n**	**Area [ha]**	**n**	**Area [ha]**
Soft clipped [25 m]	1,400	87.5	191,993	12,000
Soft clipped [2 m]	221,673	88.7	29,637,170	11,855
Hard clipped [25 m] [mask]	941	58.8	132,832	8,302
Hard clipped [2 m] [masked; based on 25 m mask]	151,280	60.5	20,745,979	8,298
Area of polygons	14	88.7	2305	11,854

3.2. Slope and S-factor [-]

Regarding slope and S-factor, both DEMs show visually almost the same properties in Frienisberg (Figure 3). In Frienisberg, the mean of slope values is 2.5% higher for the DEM2 compared to the DEM25. With 3.2% higher mean values of S-factor of the DEM2 compared to DEM25, the difference in the slope values is slightly higher (Table 5). In Lyss, the S-factor of the DEM25 has 24% lower mean values compared to the higher-resolution DEM2 or 20% lower mean values of slope regarding the different resolutions (Table 6). Also, the maximum values and standard deviation of the S-factor regarding the DEM25 are much lower than the ones of DEM2. In contrast to Frienisberg, mean and standard deviation of Lyss show lower S-factor values. In Frienisberg the mean S-factor values of DEM2 and DEM25 have lower differences than Lyss but almost the same difference of about 20% regarding the standard deviation of S-factor (Table 5, Table 6).

Table 5: Slope [°] and S-factor [-] statistics for Frienisberg, hard clipped method (masked)

Frienisberg	**Slope [2 m]**	**Slope [25 m]**	**S-factor [2 m]**	**S-factor [25 m]**
Number of cells (N)	151,280	941	151,280	941
Area [ha]	60.5	58.8	60.5	58.8
Minimum	0	0.7	0.03	0.16
Maximum	45.8	23.1	11.5	6.1
Mean	9.11	8.88	2.18	2.11
Standard deviation	4.7	3.77	1.3	1.05

Table 6: Slope [°] and S-factor [-] statistics for Lyss, hard clipped method (masked)

Lyss	Slope [2 m]	Slope [25 m]	S-factor [2 m]	S-factor [25 m]
Number of cells (N)	20,745,979	132,832	20,745,979	132,832
Area [ha]	8298	8302	8298	8302
Minimum	0	0	0.03	0.03
Maximum	65.2	45.5	14.88	11.48
Mean	3.63	2.92	0.83	0.63
Standard deviation	3.43	2.93	0.87	0.69

In Lyss the frequency analysis of the different grid resolutions shows a high amount of very low S-factor values for the DEM25 (Figure 4). For values higher than 10° the frequency is low for both resolutions. Only 7.1% (842 ha) of the agricultural area (11,855 ha) of Lyss have slope values higher than 10° and only 1.1% (130 ha) have slope values higher than 20° for the DEM2.

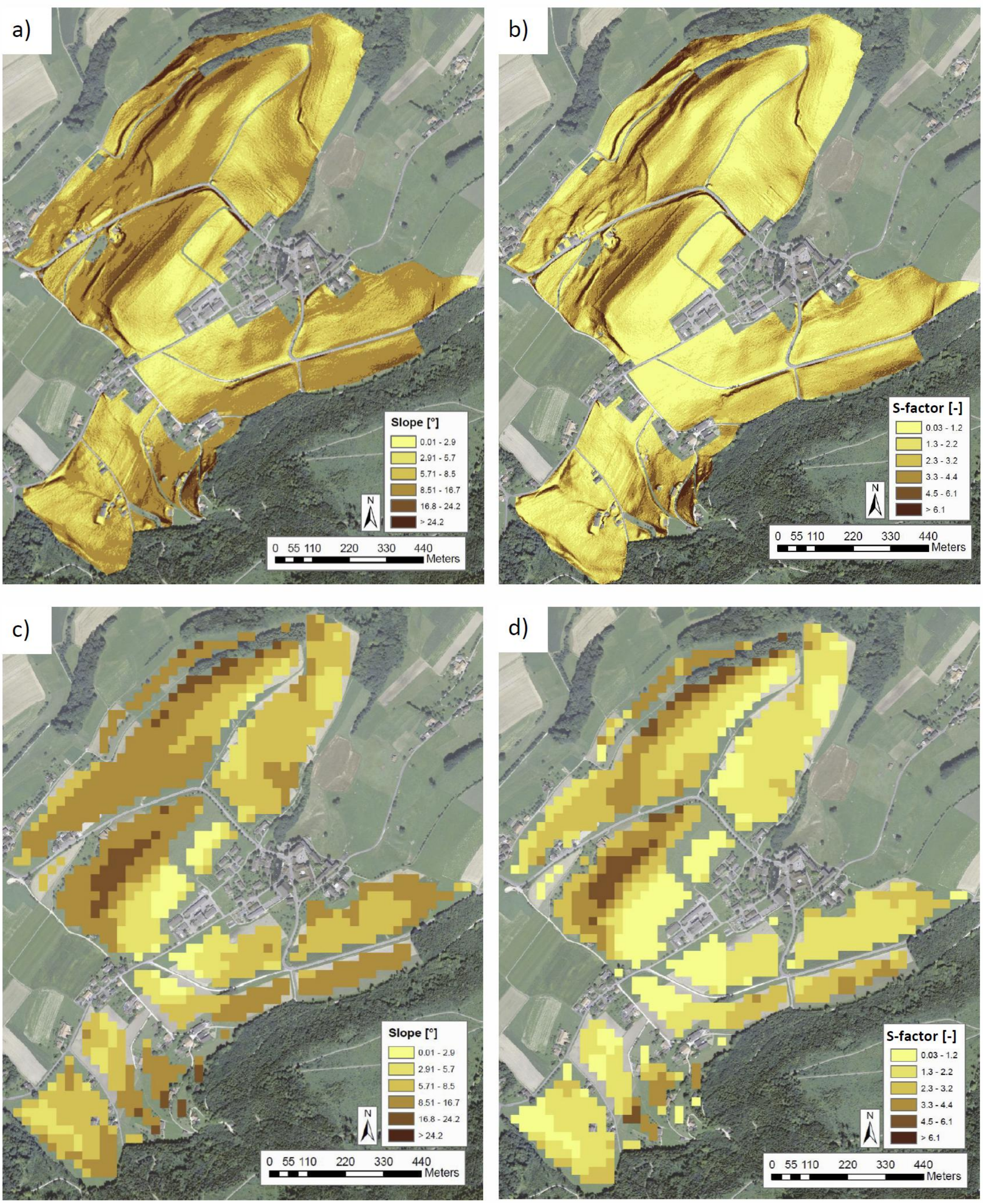

Figure 3: Topographical properties of Frienisberg; a) Slope [°] and b) S-factor [-] calculated with the RUSLE approach based on Swisstopo DEM 2015 [2 m]; c) Slope [°] and d) S-factor [-] calculated with RUSLE approach based on Swisstopo DEM 2005 [25 m]; DEM2 soft clipped; DEM25 hard clipped

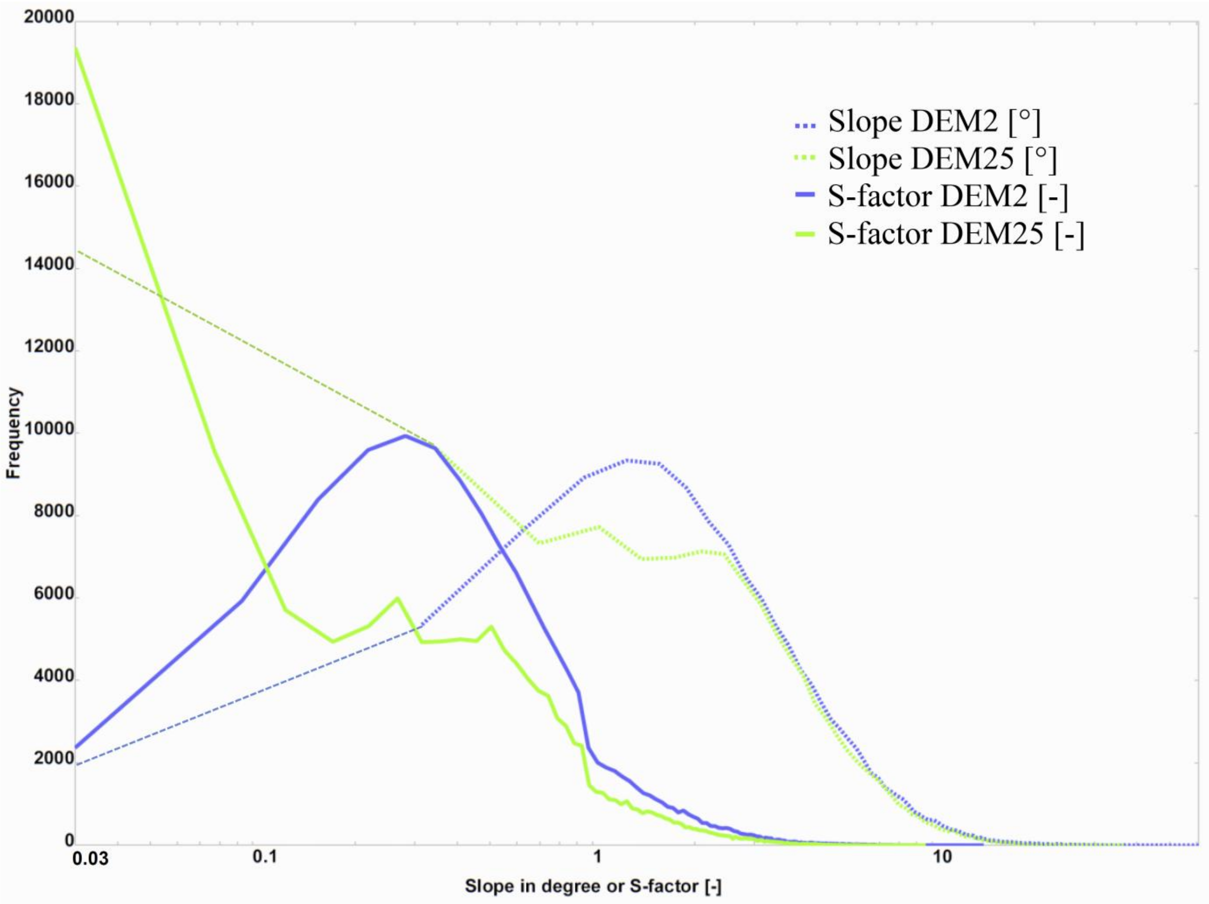

Figure 4: Frequency analysis of slope [°] (dotted lines) and S-factor [-] (solid lines) for the 2 m DEM (blue) and the 25 m DEM (green) for Lyss; hard clipped

3.3. L-factor [-]

The L-factor maps show different properties of the different MFAs in Frienisberg (e.g. Figure 5 a, d, g; low convergence values; e.g. Figure 5 c, f, i; high convergence values). The visual differences and similarities among the chosen MFAs and convergences are small. Some show more concentrated water flow properties (Figure 5; e, f, h and i corresponding to MTFD 1.1–1.25, WAT 5 and WAT 10) and some more divergent (Figure 5; a, b, c, d, g, j, k corresponding to MFD 0–1.25, MTFD 0, WAT1, DINF1.1 and MUSLE 87) water flow properties. For the DEM2, the MFA and convergence values have a low influence on the mean L-factor values (Table 7). Higher convergence values result in less dispersion of water flow, while lower convergence values lead to more dispersion. Frequency analyses of the 11 L-factors show that higher convergence values have less normal distributed frequency diagrams mainly for MTFD and WAT algorithms (Figure 6).

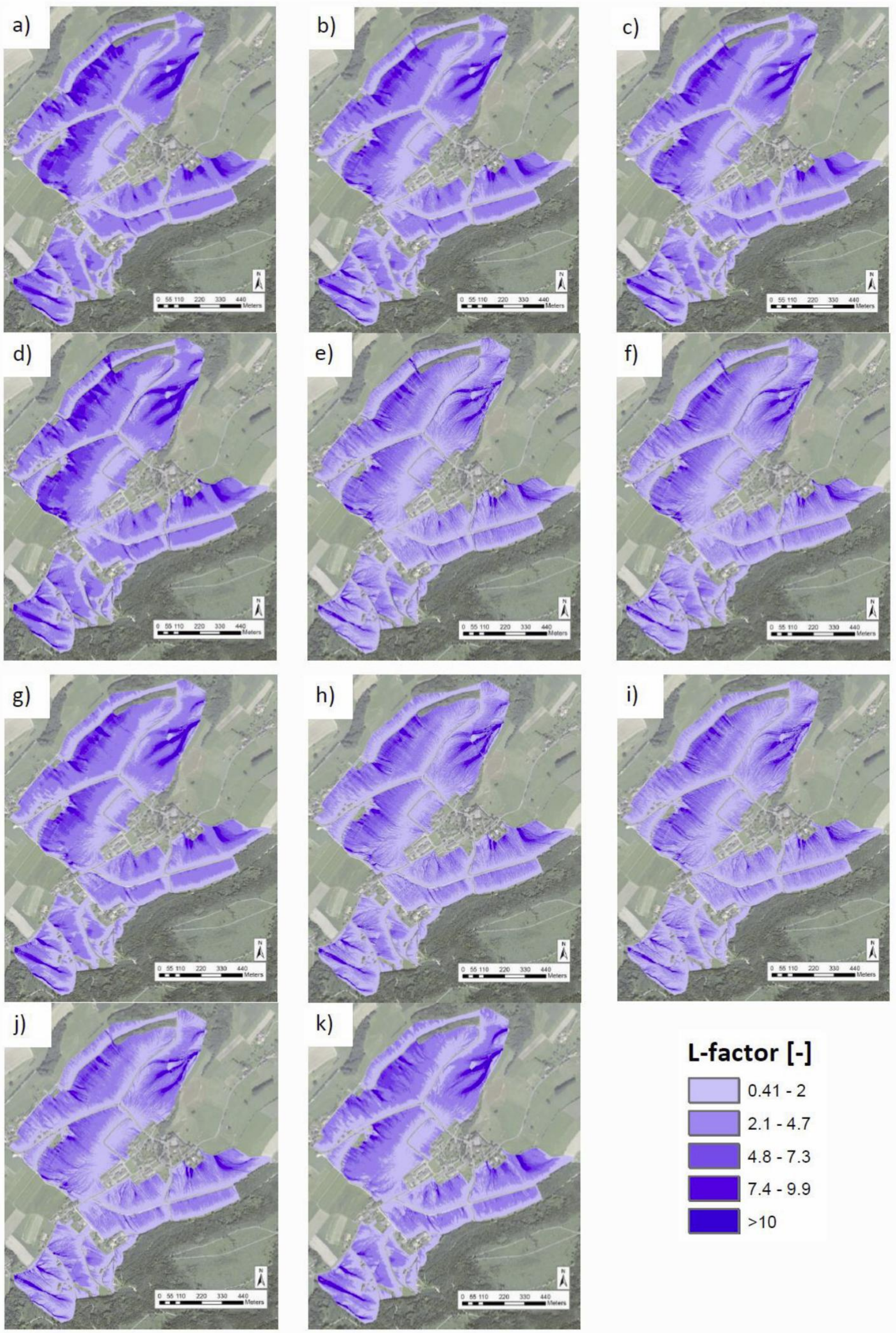
a)
b)
c)
d)
e)
f)
g)
h)
i)
j)
k)
0 55 110 220 330 440 Meters
L-factor [-]
0.41 - 2
2.1 - 4.7
4.8 - 7.3
7.4 - 9.9
>10

Figure 5: L-factor in Frienisberg calculated with 2 m resolution; a) MFD Con. Value = 0, b) MFD Con. Value = 1.1, c) MFD Con. Value = 1.25, d) MTFD Con. Value = 0, e) MTFD Con. Value = 1.1, f) MTFD Con. Value = 1.25, g) WAT Con. Value = 1, h) WAT Con. Value = 5, i) WAT Con. Value = 10, j) DINF Con. Value = 1.1, k) MUSLE 87; Con.= Convergence; soft clipped

The comparison of the 10 L-factor mean values (see Table 7, Figure 5, Figure 6) calculated with the approach of Desmet and Govers (1996) and the MUSLE 87 method (a total of 11 variations), also used in the ERM2 of Switzerland by Prasuhn et al. (2013) show very low differences in the region of Frienisberg and the DEM2 (Table 7, Figure 5, Figure 6).

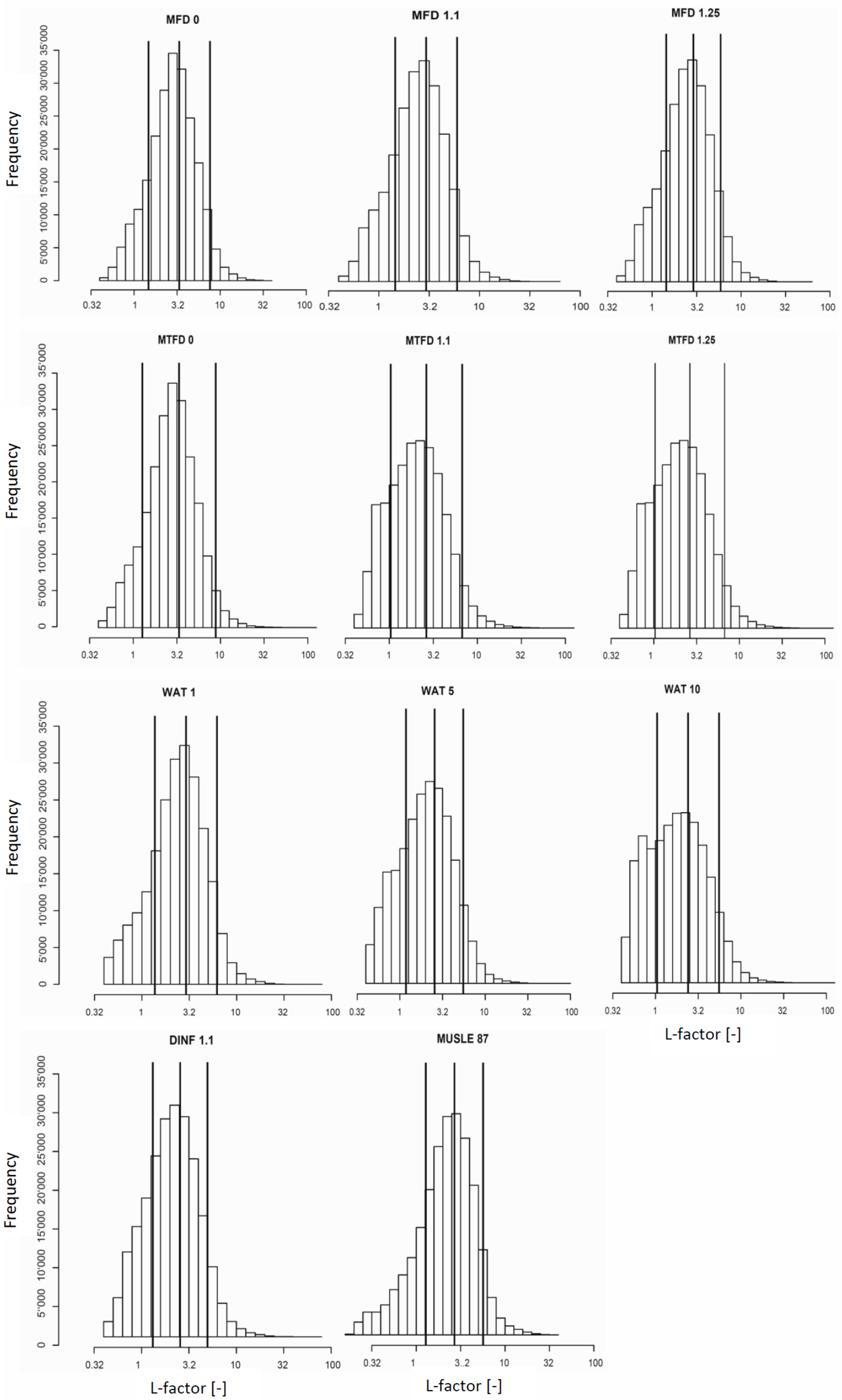
MFD 0
MFD 1.1
MFD 1.25
MTFD 0
MTFD 1.1
MTFD 1.25
WAT 1
WAT 5
WAT 10
DINF 1.1
MUSLE 87
Frequency
0
5'000
10'000
15'000
20'000
25'000
30'000
35'000
0.32
1
3.2
10
32
100
L-factor [-]

Figure 6: Frequency (y-axis) distribution of the L-factor [-](x-axis) using MFAs with different convergence values in Frienisberg for DEM2; Lines: Mean and mean ± 1* standard deviation; soft clipped

In the following, we concentrated on the MFD and on the WAT approach to compare the two tools, Saga-Gis and GrassGis. For the single field blocks in Frienisberg, the WAT algorithm shows lower mean values than MFD (Figure 7a, number of field blocks see Figure 1c), and higher convergence values lead to lower mean values, but, conversely, higher maximum values. The maximum values (Figure 7b) differ more within the MFAs, and one field block shows higher maximum values for the MFD approach compared to the WAT approach (field block 12). The field blocks 2, 3, 4, 5, 7, 9, 10, and 11 show higher maximum values for the MFD 0 compared to the WAT 1 approach. The MFD approach shows that the higher the convergence values, the more concentrated the water flows are calculated, and therefore the higher the maximum values (Figure 7b).

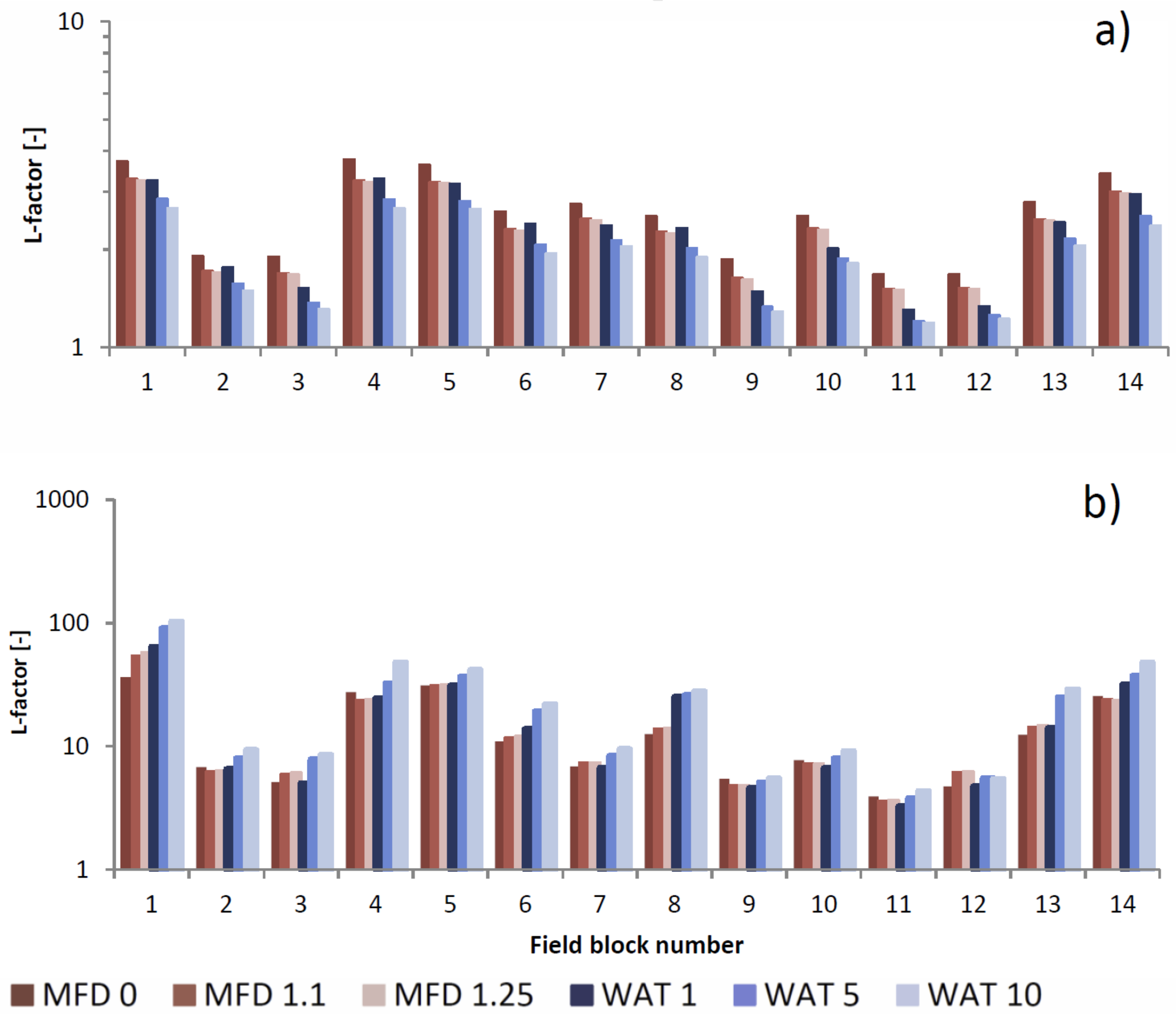

Figure 7: Mean a) and maximum b) L-factor values for selected MFD and WAT algorithms including different convergence values on 14 selected field blocks (micro-catchments [1–14, Figure 1c]) in Frienisberg with DEM2; soft clipped.

3.3.1. Effect of different resolution (2 m vs 25 m)

For the calculation of the L-factor based on the low-resolution DEM25, the clipping method applied is very important. The soft clipping method led to longer waterflow properties compared to the hard clipping method, which shows particularly clearly in the road pixels (Figure 8). The visual properties of the DEM25 also show small differences within the compared maps, but mean L-factor values are higher than using the DEM2 when a soft clipping method is applied (Table 7). The mean L-factor values calculated with SagaGis algorithms (MFD, MTFD, DINF) are 1.4–1.8 times higher and those calculated with Grass-Gis algorithms (WAT) 1.1–1.3 times higher using the DEM25 compared to the DEM2 when the soft clipping method is applied (Table 7; d). When the hard clipping method is applied, the differences are not that big, but the L-factor values using the DEM25 remain higher than those using the DEM2 (Table 7).

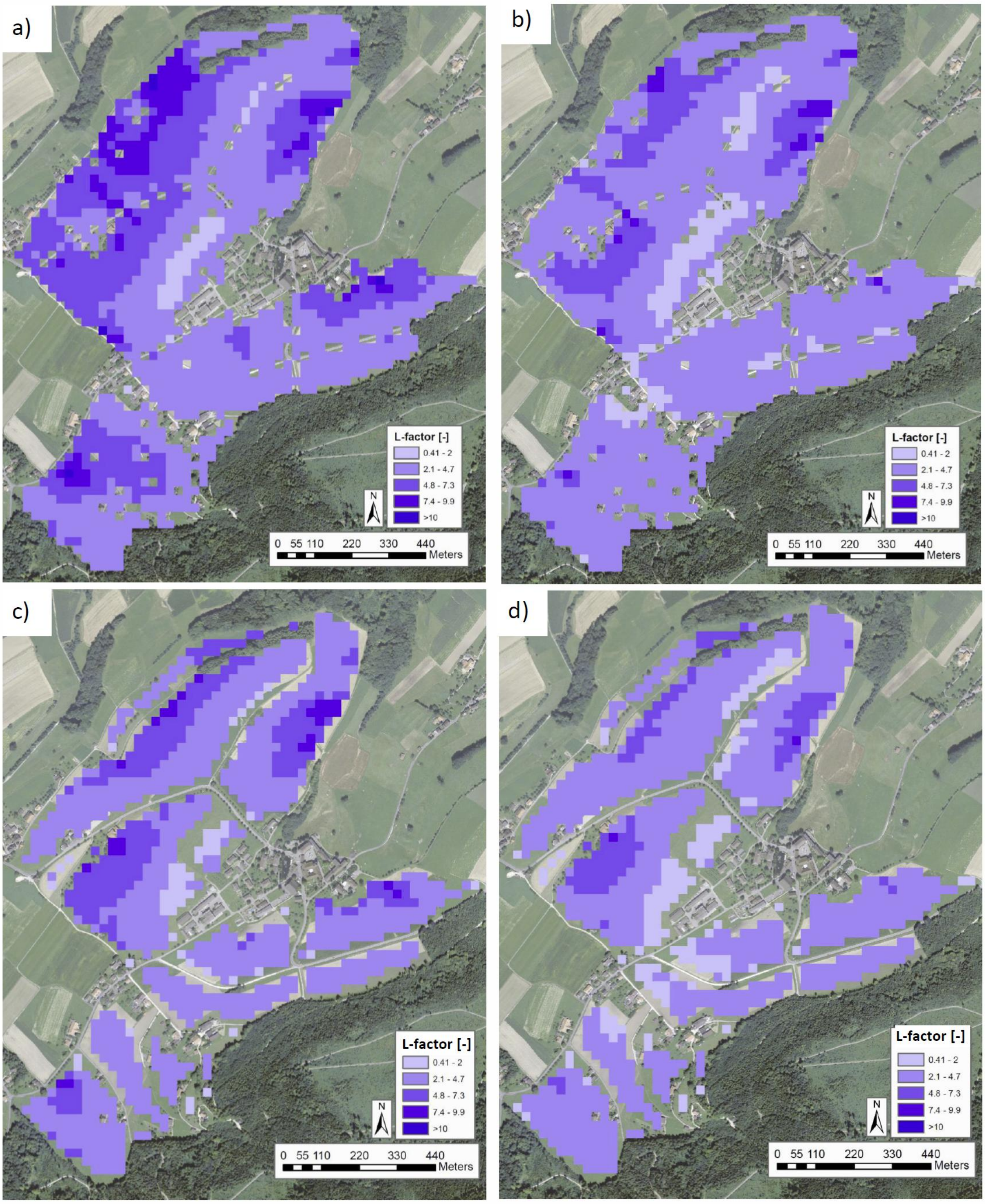

Figure 8: L-factor in Frienisberg calculated with Desmet and Govers's (1996) approach based on Swisstopo DEM (2005) with 25 m resolution; a & c = MFD Con. Value = 1.1, b & d = WAT Con. Value = 5; Con. = Convergence; a & b = soft clipped, c & d = hard clipped (masked)

Table 7: Compared MFAs and calculated resolution factor for the L-factor [-] for Frienisberg; Res. = Resolution; hard clipped (masked) only with MFD1.1 and WAT 5; No = method

No	Algorithm	MFD			MTFD			WAT			DINF	MUSLE 87
	Convergence Values	0	1.1	1.25	0	1.1	1.25	1	5	10	1.1	-
a)	Mean Res. [2 m] soft clipped	3.34	2.94	2.91	3.34	2.64	2.64	2.92	2.56	2.41	2.55	2.69
b)	Mean Res. [25 m] soft clipped	4.87	4.5	4.47	5.5	4.75	4.75	3.3	3.16	3.11	3.84	-
c)	Mean Res [25 m] hard clipped [mask]	-	3.8	-	-	-	-	-	2.8	-	-	-
d)	Res. factor: b / a	1.46	1.53	1.54	1.65	1.8	1.8	1.13	1.23	1.29	1.51	-

The boxplots (Figure 9) show that, independent of resolution, the higher the convergence values, the lower the mean and median values – which also corresponds to Table 7. There are bigger differences among the different MFA approaches (mean and median values) for the DEM25 (Figure 9a; WAT vs MFD, MTFD and DINF) than for the DEM2 (Figure 9b).

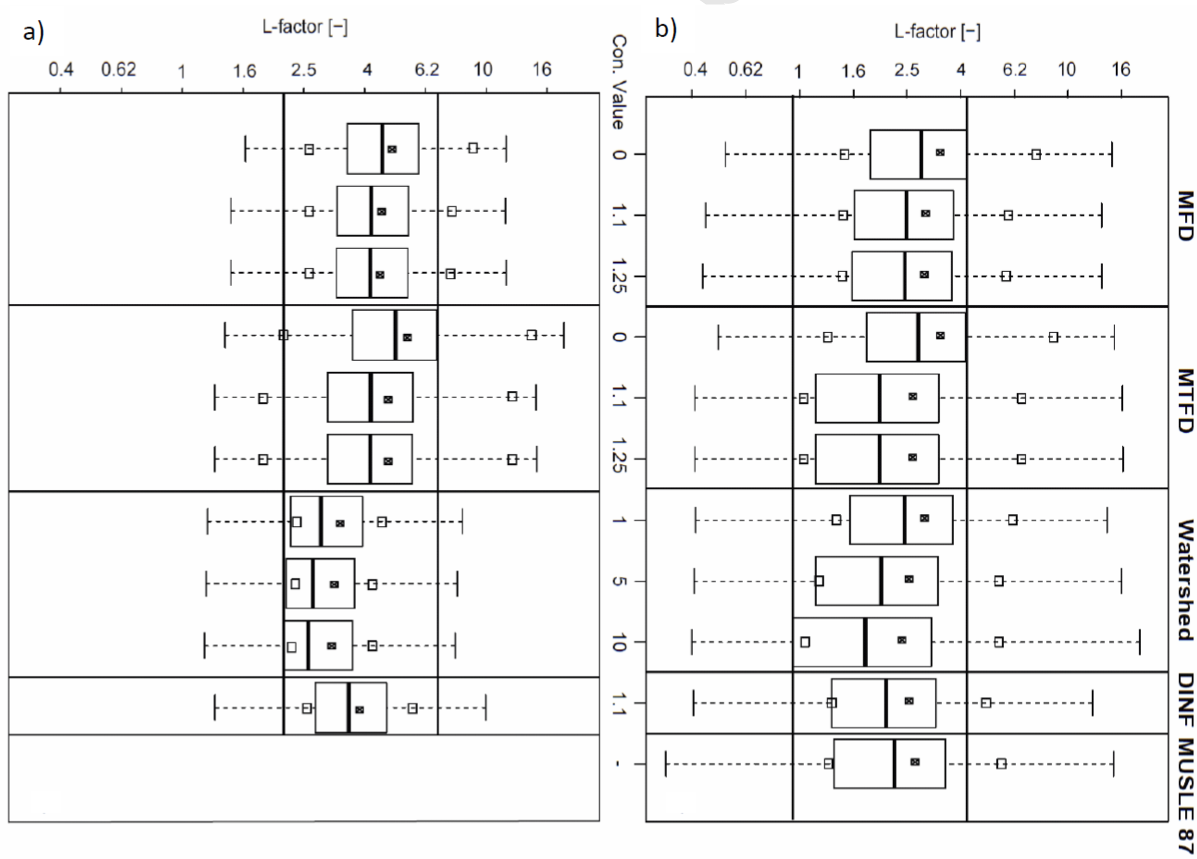

Figure 9: L-factor boxplots of different algorithms and convergence values (con. value) for Frienisberg, Square = mean ± 1 * Standard deviation, Filled dot = Mean, outliers excluded, upper horizontal line maximum of 75% quartile, lower horizontal line minimum of 25% quartile; a) Resolution: 25 m; b) Resolution: 2 m; soft clipped on both DEMs; corresponds to a and b of Table 7

In Lyss, the resolution of the DEM shows the same properties of the mean L-factor values as in Frienisberg – and both locations also show higher mean values of the DEM25 compared to the DEM2

(Table 8). But the variation of L-factor values (Minimum, Maximum, Standard deviation) are higher for the DEM2 compared to the DEM25 (Table 8).

Table 8: L-factor [-] with different resolutions and MFA approaches for Lyss; hard clipped method (masked)

L-factor [-]	MFD 1.1 [2 m]	WAT 5 [2 m]	MFD 1.1 [25 m]	WAT 5 [25 m]
Number of cells (N)	20,745,979	20,745,979	132,832	132,832
Area [ha]	8298	8298	8302	8302
Minimum	0.4	0.4	1	1
Maximum	77.5	246.4	15.0	26.5
Mean	1.60	1.71	2.24	1.87
Standard deviation	1.16	1.66	1.04	0.73

3.4. LS-factor [-]

The LS-factor was also only calculated for the algorithms MFD 1.1 and the WAT 5 (Figure 10). We reduced the number of approaches to avoid computational complexity and to consider standard convergence values only with MFD 1.1 and WAT 5. The visual comparison of both approaches for the Frienisberg region show a similar spatial distribution pattern of the LS-factors (Figure 10). The mean LS-factor in Frienisberg is higher using MFD 1.1 (= 7.8) than using WAT 5 (= 6.8) for the DEM2. It is also higher for MFD 1.1 (= 8.7) than WAT 5 (6.3) for the DEM25 (Table 9). The statistical analysis of LS-factor values of Lyss confirm the tendencies of Frienisberg. The mean values of LS-factors are a little higher for MFD 1.1 than for WAT 5 for both DEMs. In the steeper area of Frienisberg, the differences of both MFAs are more distinct compared to the more balanced area of Lyss (Table 10).

For both Frienisberg and Lyss, the descriptive statistic of the LS-factor does not show the same properties as the L-factor for the different DEMs (Table 9, Table 10). The MFD algorithm shows a slightly higher mean value for the low-resolution grid DEM25 compared to the DEM2. The WAT approach shows the opposite: a higher mean value of the WAT approach with DEM2 compared to DEM25. The higher tendency of mean L-factor value comparing the DEM25 (1.87) with the DEM2 (1.71) decreases after multiplication with the S-factor for the WAT approach in Lyss (LS-factor: DEM25: 1.5; DEM2: 1.76; Table 8, Table 9, Table 10).

For Lyss, Figure 11 shows percentages of area for slope, S-factor, L-factor, and LS-factor for defined categories calculated with MFD 1.1 for DEM2 and DEM25. Classes with values > 1.2 of S-factor include a considerably higher area of 22% for the DEM2 compared to 14% for the DEM25. Notably, very high values hardly occur in the DEM25. L-factors with very high values > 7.3 occur much more frequently in the DEM2 than in the DEM25. But even in the lowest L-factor class (0.41–2) there is a larger area proportion in the DEM2 than in the DEM25. This partly compensates high S-factor values with low L-factor values in the DEM2, except for the highest values. Therefore, the LS-factor classes have similar values in the different resolutions except in the two highest classes (Figure 11). In class >30 the percentage of area is three times higher for the DEM2 compared with the DEM25.

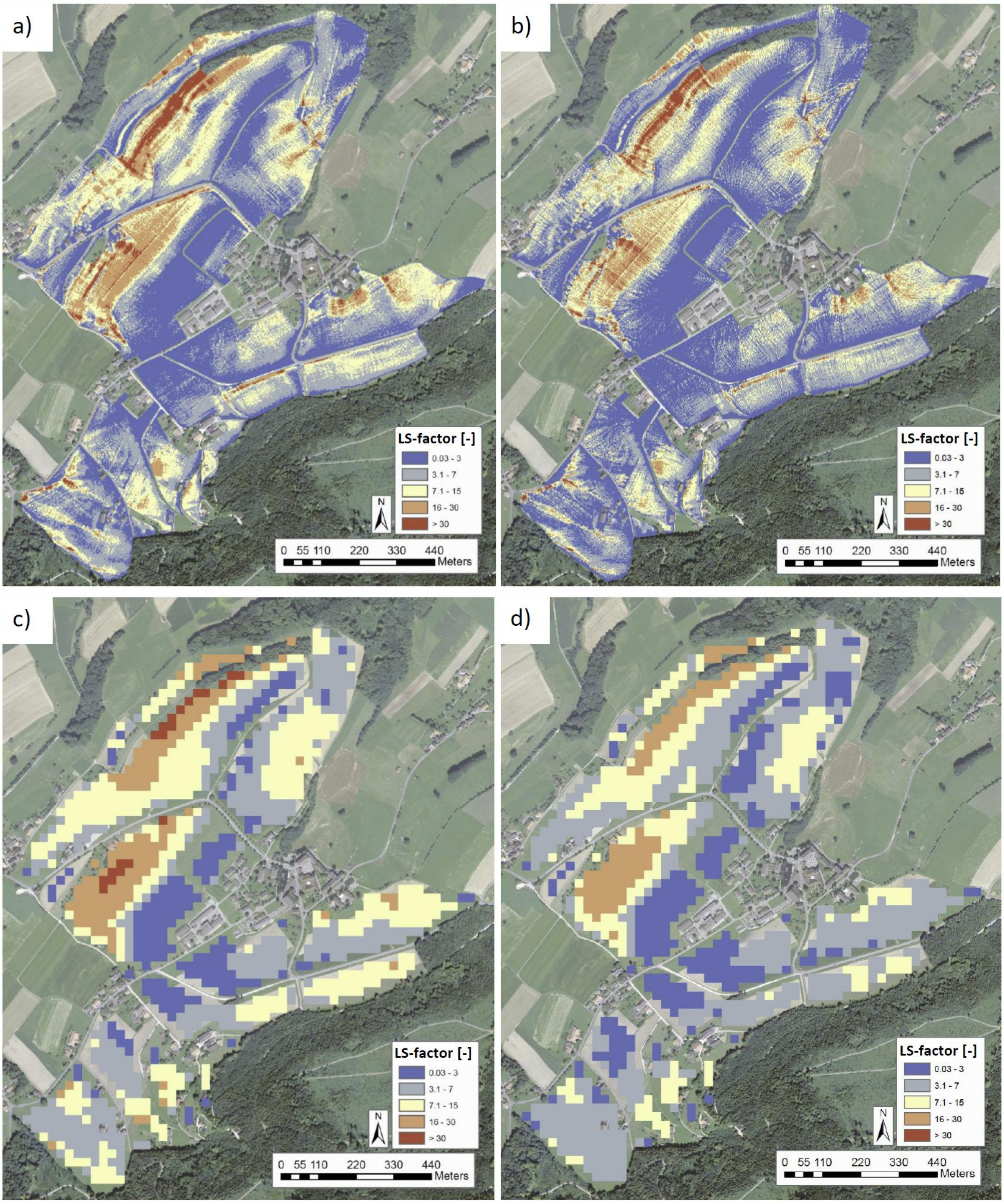

Figure 10: LS-factor [-] multiplied based on approaches of L- and S-factor [-] a & c = MFD 1.1, b & d = WAT 5, a & b [2 m], c & d [25 m] in Frienisberg; DEM2 soft clipped; DEM25 hard clipped (masked)

Table 9: LS-factor [-] statistic of two different algorithms and resolutions calculated for Frienisberg; hard clipped method (masked)

LS-factor [-]	MFD 1.1 [2 m]	WAT 5 [2 m]	MFD 1.1 [25 m]	WAT 5 [25 m]
Number of cells (N)	151,280	151,280	941	941
Area [ha]	60.5	60.5	58.8	58.8
Minimum	0.03	0.03	0.03	0.03
Maximum	450	746	39.9	29.9
Mean	7.8	6.8	8.7	6.3
Standard deviation	8.4	8.21	6.9	5.1

Table 10: LS-factor [-] statistic of two different algorithms and resolutions calculated for Lyss; hard clipped method (masked)

LS-factor [-]	MFD 1.1 [2 m]	WAT 5 [2 m]	MFD 1.1 [25 m]	WAT 5 [25 m]
Number of cells (N)	20,745,979	20,745,979	132,832	132,832
Area [ha]	8298	8298	8302	8302
Minimum	0.03	0.03	0.03	0.03
Maximum	450	1308	68	59
Mean	1.79	1.76	1.88	1.50
Standard deviation	3.20	3.50	2.83	2.06

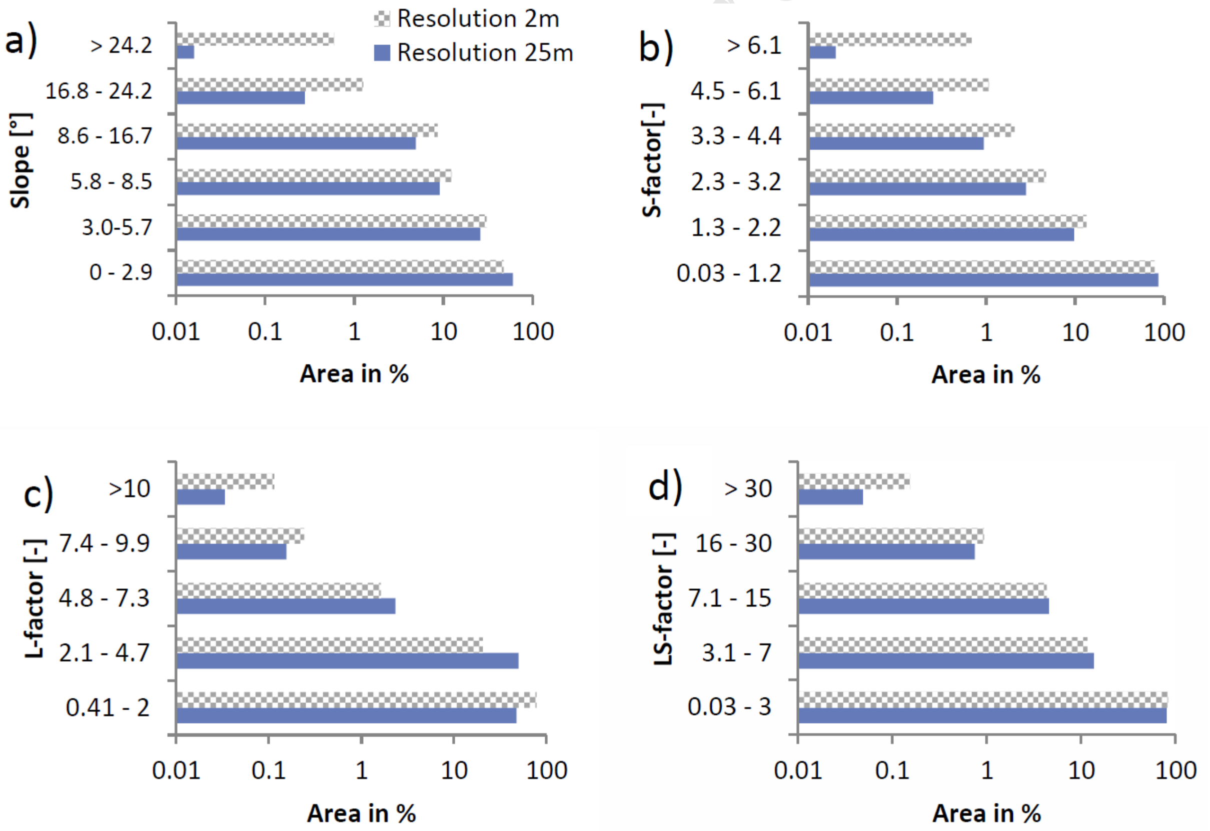

Figure 11: Percentage of area in different categories of Slope a), S-factor b), L-factor (MFD 1.1) c), and LS-factor (MFD 1.1) d) for Lyss; hatched bar = resolution of 2 m; blue bar resolution of 25 m; hard clipped method (masked); the classes selected for the y-axes are not or only to a limited extent comparable among Slope, S-factor, L-factor, and LS-factor

To consider the big influence of field blocks for the LS-factor calculation, we computed the LS-factor without field blocks in Lyss based on the DEMs without any flow barriers. Using the MFD algorithm with the convergence value 1.1, the mean LS-Factor values for Lyss without field blocks are 70%

higher (with field blocks 1.88, without 6.36) for the DEM25 and 49.7% higher (with field blocks 1.79, without 3.56) for the DEM2. Table 11 summarizes the main results.

Table 11: Overview of the main results (mean values of L- and LS-factor for the 2m and 25m grid) for Frienisberg (lightly shaded) and Lyss (strongly shaded)

Tool	**Algorithm**	**Convergence value**	**L-factor[1] Soft clipped**		**L-factor[1] Hard clipped**		**LS-factor[2] Hard clipped**	
			2m	25m	2m	25m	2m	25mx
Saga Gis	**MFD**	0	3.34	4.87	-	-	-	-
		1.1	2.94	4.5	3.24	3.8	7.8	8.7
					1.60	2.24	1.79	1.88
		1.25	2.91	4.47	-	-	-	-
	MTFD	0	3.34	5.5	-	-	-	-
		1.1	2.64	4.75	-	-	-	-
		1.25	2.64	4.75	-	-	-	-
GrassGis	**WAT**	1	2.92	3.3	-	-	-	-
		5	2.56	3.16	2.85	2.8	6.8	6.3
					1.71	1.87	1.76	1.5
		10	2.41	3.11	-	-	-	-
Saga Gis	**DINF**	1.1	2.55	3.84	-	-	-	-
AVErosion in ArcView	**MUSLE 87**	-	2.69	-	-	-	-	-

[1] Calculated according to Desmet & Govers 1996
[2] Product of L- and S-factor
Lightly shaded: Frienisberg; strongly shaded: Lyss
- = not calculated or not available

MFD: Freeman 1991; MTFD: Seibert and McGlynn 2007; WAT: Ehlschlaeger 1989, Quinn et al. 1991; DINF: Tarboton 1997; MUSLE 87: Moore and Burch 1986, Moore et al. 1991

4. Discussion

4.1. Digital elevation model (DEM) correction and hydrological connectivity

A correction of the digital terrain model is especially necessary for high-resolution terrain models and use of multiple flow algorithms (Liu et al. 2015; Yang 2015). The aim of partial sink filling (with 0.5 m, Table 3) was to eliminate small sinks and artefacts, but allow that larger sinks or depressions in the terrain are not necessarily connected. Flow sinks are real existing drainless sinks or plains and are not the result of vertical errors of the DEM. Thomas et al. (2016) showed that flow sinks are widespread and 16 - 33% of catchment areas are hydrologically disconnected from the aquatic network. In Lyss, the correction of the DEM does not have a big influence: because of the varied topography absolute sinks are large and would need high fill heights (> 4 m; Table 3) to balance them. At the selected filling level of 0.5 m, only in 4% of the area, the DEM is corrected and sinks are filled such that the water flow through those areas is connected. The fill height value 0.5 m also covers the accuracy of ± 0.5 m 1 σ of the DEM (SwissALTI3D 2015).

The field block map leads to differences between the DEM25 and the DEM2 due to clipping inaccuracies. Owing to the small size of the field blocks (mean value of 5 ha), there is an undesirable edge effect, especially with the DEM25. Small roads or other objects preventing a continuous water flow were sometimes not respected in the 25 m grid during the soft clipping method. This leads to higher slope lengths or slope contributing areas, and also to higher L-factor mean values using the DEM25 MFAs compared to the DEM2 MFAs (Table 7, Figure 8). When hard clipping is applied peripheral areas are sometimes lost. In addition, flow barriers like forests and small streets are not necessarily flow barriers in every situation (Volk et al. 2010). During heavy rains those areas can act as external water sources and are therefore not considered in the field block map approach also mentioned in Prasuhn et al. (2013).

Soft clipping without mask is the standard method to receive most of the raster information and will be used for the calculation of the new erosion risk map (ERM) of Switzerland with the two-metre

DEM. For this high-resolution DEM, the clipping method is not that important and data loss due to the clipping method is negligible (0% in Frienisberg and 0.01% for Lyss) (Table 4).

4.2. S-factor approaches

Comparing different S-factor approaches for slope values higher than 10° lead to big differences (Figure 2). Very high slope values do not appear very often, so the effect of slopes higher than 10° is not very strong for Lyss (Figure 4). The RUSLE approach shares with other widely used approaches similar S-factor values (e.g. Zingg 1940; Hurni 1979; Nearing 1997; see) up to a slope steepness of 10°. Some S-factor approaches are only extrapolated and not measured on slope values higher than 11.3° (Hurni 1979; Liu et al. 1994). Most of the slope values (98.9%) in the study area are below 20° (Lyss), where most of the nine S-factor approaches do not show big differences (Figure 2). Hrabalíková and Janeček (2017) compared four different S-factor approaches and concluded that the values of the S-factor are within a similar range and that there is no significant difference. Thus, the choice of S-factor calculation for our purposes does not have a big influence. In the selected approach (RUSLE after Renard et al., 1997), however, there are large differences in the calculated S-factors, depending on the resolution of the DEM used. The DEM25 leads to significantly lower S-factors due to smoothing effects, both in mean values as well as in the maximum values and standard deviation (Table 5, Table 6, Figure 11). This is in line with findings in other studies (Di Stefano et al. 2000, Kienzle 2004). In terms of soil erosion, this means that with increasing DEM resolution, the S-factors increase and thus also soil erosion.

4.3. L-factor approaches

The MFAs do not differ very much regarding the L-factors and the mean values of the default convergence options with MFD 1.1, MTFD 1.1, WAT 5, DINF 1.1, and MUSLE 87 in Frienisberg and the DEM2 (Figure 5, 6, 9). Between the highest of the default convergence options (MFD 1.1 = 2.94) and the lowest (DINF 1.1 = 2.55), mean L-factor values vary only about 13%. Compared with the highest and lowest convergence options of the MFA (MFD 0 = 3.34, MTFD 0 = 3.34, and WAT 10 = 2.41) the difference is 28% in Frienisberg (Table 7). For the DEM25 the default convergence options and soft clipped approach show a difference of 33% between the highest L-factor value (MTFD 1.1 = 4.75) and the lowest one (WAT 5= 3.16). Comparing the mean L-factor values of the highest and lowest convergence options (MTFD 0 = 5.5, WAT 10 = 3.11) the difference is 43% in Frienisberg when the soft clipped approach is applied (Table 7). For both DEMs, the higher the convergence values of MFA, the lower the mean values of the L-factor. Comparing masked (hard clipped) and not masked (soft clipped) approaches in Frienisberg of the DEM25, the differences between MFD 1.1 (3.8 vs 4.5) are 16% and 11% for WAT 5 (2.8 vs 3.16) but have still higher mean L-factor values compared to the DEM2 (Table 7). In Lyss the differences of mean L-factor values are low for both DEMs, but also higher for the DEM25 than the DEM2. The L-factor of MFD 1.1 and WAT 5 showed a mean of 1.6 and 1.71 (DEM2) – i.e. 28% and 9% lower than with the DEM25 (mean values 2.24 and 1.87) (Table 8).

The use of multiple flow algorithms rather than single flow algorithms has now become an established method in most water flow or soil erosion modelling studies (Mitasova et al. 1996; Panagos et al. 2015a, b; Zhang et al. 2017). Wilson et al. (2008) compared the hydrological performance of various flow-routing algorithms and found that the single flow direction method produced more 'low flow' cells. Orlandini et al. (2012) showed that the multiple flow direction method performed best at very high DEM resolutions. Multiple flow direction algorithms can accommodate convergent and divergent flow and perform better than single flow direction method algorithms for real terrains. But it is not easy to evaluate the performance of the algorithms with field observations. Accordingly, there are hardly any such studies. Most of them are based on visual or qualitative assessments and recommend the algorithms used based on "goodness-of-fit" (Wilson et al., 2008). We too can only perform such a qualitative assessment in this study.

It is questionable whether the empirical relationships between the LS factor and the soil erosion risk underpinning RUSLE can be downscaled or upscaled from the size of standard USLE plots (22.1 m) to the 2 m or 25 m grid or even other grid resolutions. The adjustment of the slope length factor L on the basis of the calculation of the contributing area with MFAs may also be questioned. The observed rill and ephemeral gully erosion (thalweg erosion) is represented well but extending RUSLE beyond its empirical limitations (Prasuhn et al. 2013). The approach with MFA and high-resolution DEM of our study is actually used today as a standard method in GIS-based modelling. Whether this procedure is permissible or not is not the aim of this study.

4.4. LS-factor approaches

Comparing the LS-factors calculated with MFD 1.1 and WAT 5 using DEM2 for Frienisberg and Lyss, there are no big differences between the two algorithms (Figure 10, Table 9, Table 10). In Lyss, the mean LS-factor is slightly higher (+ 2%) using the MFD 1.1 (1.79) than using the WAT 5 (1.76). The deviation of the values is greater (+ 9%) for WAT 5, where standard deviation was 3.50 compared to 3.20 for MFD 1.1. When we compare the two MFAs using the DEM25, the difference is higher. The mean LS-factor for the MFD 1.1 (1.88) is higher than for WAT 5 (1.50) (+ 25%). In addition, MFD 1.1 generates higher standard deviation and maximum values compared to WAT 5. In the smaller and steeper Frienisberg area, similar differences between the two MFAs result, but these are somewhat more accentuated (Table 9, Table 10).

For Frienisberg, the LS-factor of the lower-resolution DEM25 has a higher mean value than the DEM2 for the MFD approach, but a lower mean value when using the WAT approach (WAT: - 7.4%; MFD: + 11.5%) and in Lyss (WAT: - 14.7%; MFD: + 5%; Table 9, Table 10) Other studies (Claessens et al. 2005: 10–100 m; Wu et al. 2005: 10–250 m; Mondal et al. 2017: 30–330 m) show lower mean values using the low-resolution DEM compared to the high-resolution DEM, but do not consider DEMs with resolutions higher than 10 m. Deumlich (2012) compared different resolutions (1–25 m), modelling, on two field blocks of 69/141 ha, an average soil loss of 1.2/1.4 t ha^{-1} using DEM2 and 0.75/0.99 t ha^{-1} using DEM25. The average potential soil loss is doubled, from the highest resolution grid (1 m) to the coarsest (25 m). In a study in northern China, Wang et al (2016) compared grid sizes of 2, 5, 10, 25, and 30 m, and used the 2 m resolution grid as a reference to calculate soil loss. They reported a decrease of 47% with a 30 m DEM, and said the DEM2 is the most accurate in describing the topography and the micro-relief. Fu et al. (2015) [2–30 m] reported that LS-factor of 10 m resolution DEM were close to the values of 2 m resolution DEM. Koo et al. (2016) obtained similar results to those in our study with lower mean values for a 5 m grid compared to a 20 m grid, but higher mean values for a 30 m grid. This corresponds to a break between 20–30 m and also includes the standard plot size of RUSLE estimation of 22.1 m (Wischmeier and Smith 1978; Renard et al. 1997). Bhattarai and Dutta (2007) highlight that the better results of the 30 m resolution compared to the 90 m using the USLE methodology, is probably due to fact this resolution is closer to the 22.1 m slope length, the length used in the derivation of the USLE relationships.

In Lyss, 99.8% of calculated LS values were < 30, 98.9% < 15, and 83.1% < 3 for the DEM2. For the DEM25, 99.9% of calculated LS values in Lyss were < 30, 99.2% < 15, and 81% < 3 (Figure 11). We compared LS-factors calculated with Equation 2-4 with the LS-factor values of the tables 4.1-4.3 in the main reference RUSLE handbook of Renard et al. (1997) based on 122 m slope length. These RUSLE tables 4.1-4.3 represent LS-factor values for uniform slopes. Table 4.1 is used for rangeland and pasture with a low interrill/rill ratio. Table 4.2 is used for cropland and pasture with a moderate interrill/rill ratio and Table 4.3 for construction sites with high ratio of interrill and rill (Renard et al. 1997). For slopes up to 3% the differences between the calculated values and the indicated values in the tables were relatively small (average deviation between 4-24%), depending on the used RUSLE table (4.1-4.3). For slopes between 3- 15% our approach always resulted in slightly higher LS-values (average deviation 10-49%) compared to the RUSLE tables (4.1-4.3). For slopes greater than 15%, which account for less than 1% of the total area (Figure 11), the deviation (average deviation between 24-55%) from our approach increased with increasing slope compared to the RUSLE –tables 4.1-4.3 (Renard et al. 1997). Yang (2015) calculated for New South Wales, Australia, a similar distribution of LS-factor values as in our study. The LS-values range from 0.05 to 60 with a mean of 2.60 based on a 30 m resolution DEM. Nearly all (99%) of the calculated LS values are < 30, 80% < 10, and 30% < 1.0. Very high L- and LS-factor values of single pixels are quite justified. Those pixels occur mainly in terrain depressions, where a lot of water can flow together and the upslope contributing area is very big. In those areas, very high soil loss values are manifested as rills or thalweg erosion (Prasuhn 2011). Deumlich (2012) compared RUSLE models with measured soil losses and concluded that the DEM25 is insufficient to illustrate small-scale erosion phenomena. Even the results of DEM10 and DEM5 reflect the properties of erosion only in a simplified manner in the mentioned case. But flow paths are well represented using DEM1. Gertner et al. (2002) reported that DEMs with resolutions lower than 5 m are not suitable for the calculation of LS-factors due to large variations in upslope contributing areas. Thomas et al. (2017) reported that optimal DEM resolutions of hydrologically sensitive areas are between 1–2 m. Unlike the previously mentioned studies, one other study implies higher mean LS-factor values regarding the 10 m and 20 m resolution DEM compared to the 5 m resolution DEM on watersheds in Korea (Koo et al. 2016).

The chosen approach with field blocks as micro-catchments of 5 ha mean area as a basis for calculating LS-factors is only very suitable for high-resolution DEMs, such as the DEM2 used here. In coarser-resolved DEMs, clipping effects lead to large uncertainties and errors. When using DEM2, however, the chosen approach with the micro-catchment has many advantages. The problem of the maximum slope length or maximum number of pixels of the upslope contributing area, which is frequently discussed in the literature, does not exist. Several other problems are also elegantly bypassed, e.g. the need for complex models to identify breaks in slope length that involve changes in the slope turning point; the challenge of enabling variable cut-off slope angles; and the challenge of adequately considering channel networks to locate soil erosion and deposition zones (Van Remortel et al. 2001; Liu et al. 2015; Yang 2015; Zhang 2017). Maximum slope length value (e.g. 305 m; Renard et al. 1997) is already respected with the field block approach. Also, the channel network is already included and does not have to be additionally separated. Borrelli et al. (2016) used a similar approach as in our study. They used remote sensing techniques to introduce the “field boundaries/channelled flow concept” in a national-scale RUSLE application for Italy. The DEM25 was previously segmented to represent some potential man-made or natural structures, e.g. agricultural canals, roads, soil furrows, or gullies. Maugnard et al. (2013) also performed a soil erosion risk map of Wallonia (Belgium) with 10 m pixel resolution based on hydrologically isolated plots similar to the applied field block approach in this study. Our comparison of calculated LS-factors with or without field block map shows that massively higher mean LS-factors result (3.56 vs 1.79) if the whole area is considered as a homogeneous landscape without barriers. Winchel et al. (2008) compared different LS-factor calculations with and without terrain barriers and a cut at 333 m slope length and a 30 m DEM of 40 hydrologic units in the USA and confirm our observation in their analysis.

It could be pointed out that the use of various algorithms for detecting the LS-factor remains a subject of controversial discussions despite numerous new developments, GIS technologies, and better computing capacity (Mitasova et al. 2013; Oliveira et al. 2013; Hrabalíková and Janeček 2017). Desmet and Govers (1996) stated that the LS values predicted by the GIS method are generally higher by 10–50% than those obtained by manual approach. In contrast, Hrabalíková and Janeček (2017) found that the LS values generated by the GIS method were generally 10–30% lower than those obtained by the manual method. These findings are in agreement with the conclusions of Yitayew et al. (1999) stating that the mean annual erosion was mostly under-predicted by the GIS methods. Garcia Rodriguez and Gimenez Suarez (2010) observed an overestimation in the values of the LS-factor, when it is calculated in the traditional way. Hrabalíková and Janeček (2017) conclude that the GIS-based RUSLE soil loss estimates from five of seven different approaches to calculation of LS-factor are lower than the measured average annual soil loss and two approaches over-predicted the measured soil loss.

5. Conclusion and Outlook

To calculate the L-factor of the RUSLE, we compared four different multiple flow direction algorithms (DINF, MFD, MTFD, WAT) with different convergence settings and the previously used MFA (MUSLE 87) of the existing erosion risk map in Switzerland. We performed this comparison with a high-resolution DEM2 and a coarser DEM25 in two different test areas in the Swiss Plateau, based on previously segmented micro-catchments of variable spatial dimension with a mean size of 5 ha. In total, we performed 21 different L-factor calculations. Selected approaches were calculated with the S-factors to obtain the LS-factors.

In terms of L-factor values, the MFAs tested in both areas using the DEM2 did not differ considerably. The L-factor values also did not differ much from those obtained in the approach used for the current erosion risk map (ERM2). As the convergence values increases, the mean L-factors decrease slightly in all MFAs. The choice of the MFA does not play a big role in the calculation of the soil erosion risk in DEM2 in our area, and there is no big difference to the approach used for the ERM2. With the DEM25, notably lower mean L-factors are calculated with WAT than with MFD, MTFD, and DINF. Surprisingly, L-factors calculated using the DEM25 are slightly higher for all MFAs than for the same MFAs when using the DEM2. Regarding the S-factors, however, smoothing effects in the coarser DEM25 lead to lower values compared to those calculated using the DEM2.

For the LS-factor calculation, only the two approaches MFD 1.1 and WAT 5 were compared for both DEMs. The MFD 1.1 and WAT 5 differ only slightly on the DEM2. Comparing the two DEMs gives an ambivalent picture. MFD 1.1 produces lower mean LS values on the DEM2 than on the DEM25, whereas WAT 5 produces higher values for the DEM2 than the DEM25. With the 25 m model, hard clipping results in a considerable loss of data at the edges of the field blocks. This is not so important for the calculation of S and L-factors and mean values, but would lead to a significant underestimation of soil loss when calculating absolute soil loss rates. With soft clipping, the data loss on the DEM25 is lower, but the slope lengths and thus the L-factor increase. This would lead to an overestimation of the soil loss. The DEM25 is therefore unsuitable for the chosen approach with field blocks (micro-catchments averaging 5 ha).

We do not have experimental data to evaluate the results of the 21 L-factor variations. Therefore, we cannot say what is more convenient, but we can make a qualitative assessment and point out differences. The low influence of the different MFAs and the convergence options on the L- and LS-factor calculations came as a surprise, but are confirmed by our study. Furthermore, our results do not confirm the hypothesis that a higher DEM resolution leads to higher L-, S-, and LS-factor values. In a subsequent study, the various chosen LS-factors will be calculated with the other factors of the RUSLE (R, K, C, P factor) in the Frienisberg region to calculate the actual soil erosion risk for each plot and compared it with long-term measured soil loss from field data on soil erosion damage mapping of a monitoring program (Prasuhn 2011, 2012). The LS-factor approach that best reflects the reality is then applied and will be used to validate and fine-tune the RUSLE model for the new erosion risk map of Switzerland.

Although the influence of the resolution of the DEM on mean LS-factor values is not very big, it is very important for the characterization of a land surface in terms of concavity and complexity. The spatial distribution in the DEM2 is varied and much more differentiated and better represents reality. This is crucial for the credibility of an erosion risk map to farmers, consultants, and advisors, as well as for the targeted planning of mitigation measures.

Acknowledgments

This research is part of a soil erosion risk project, funded by the Swiss Federal Office for Agriculture (FOAG). We also thank Tina Hirschbuehl[1] and Marlène Thibault[1] (CDE) for the English editing support.

References

Abu Hammad, A., Lundekvam, H., Børresen, T., 2004. Adaptation of RUSLE in the eastern part of the mediterranean region. Environmental Management 34, 829–841.

Alder, S., Prasuhn, V., Liniger, H., Herweg, K., Hurni, H., Candinas, A., Gujer, H.U., 2015. A high-resolution map of direct and indirect connectivity of erosion risk areas to surface waters in Switzerland: A risk assessment tool for planning and policy-making. Land Use Policy 48, 236–249.

Arge, L., Chase, J. S., Halpin, P., Toma, L., Vitter J. S., Urban, D., Wickremesinghe, R., 2003. Efficient flow computation on massive grid terrain datasets. GeoInformatica 7, 283-313.

Auerswald, K., 1987. Sensitivität erosionsbestimmender Faktoren. – Wasser und Boden 1, 34-38.

Benavidez, R., Jackson, B., Maxwell, D., Norton, K., 2018. A review of the (Revised) Universal Soil Loss Equation (R/USLE): with a view to increasing its global applicability and improving soil loss estimates. Hydrology and Earth System Sciences Discussions, 1-34.

Bhattarai, R. and Dutta, D., 2007. Estimation of soil erosion and sediment yield using GIS at catchment scale. Water Resources Management 21, 1635–1647.

Boardman, J., 2006. Soil erosion science: Reflections on the limitations of current approaches. Catena 68, 73-86.

Böhner, J. and Selige T., 2006. Spatial prediction of soil attributes using terrain analysis and climate regionalisation. Göttinger Geographische Abhandlungen 115, 13–28.

Boomer, K. B., Weller, D. E., Jordan, T. E., 2008. Empirical models based on the universal soil loss equation fail to predict sediment discharges from Chesapeake Bay catchments. Journal of Environmental Quality 37, 79-89.

Borrelli, P., Meusburger, K., Ballabio, C., Panagos, P., Alewell, C., 2018. Object-oriented soil erosion modelling: A possible paradigm shift from potential to actual risk assessments in agricultural environments. Land Degradation and Development 29, 1270-1281.

Borrelli, P., Paustian, K., Panagos, P., Jones, A., Schütt, B., Lugato, E., 2016. Effect of good agricultural and environmental conditions on erosion and soil organic carbon balance: a national case study. Land Use Policy 50, 408-421.

Borrelli, P., Robinson, D. A., Fleischer, L. R., Lugato, E., Ballabio, C., Alewell, C., Meusburger, K., Modugno, S., Schütt, B., Ferro, V., Bagarello, V., Oost, K.V., Montanarella, L., Panagos, P., 2017. An assessment of the global impact of 21st century land use change on soil erosion. Nature Communications 8, 1-13.

Claessens, L., Heuvelink, G. B. M., Schoorl, J. M., Veldkamp, A., 2005. DEM resolution effects on shallow landslide hazard and soil redistribution modelling. Earth Surface Processes and Landforms 30, 461–477.

Costa-Cabral, M. and Burges, S. J., 1994. Digital Elevation Model Networks (DEMON): a model of flow over hillslopes for computation of contributing and dispersal areas. Water Resources Research 30, 1681-1692.

Desmet, P. J. J. and Govers, G., 1996. A GIS procedure for automatically calculating the USLE LS factor on topographically complex landscape units. Journal of Soil and Water Conservation 51, 427-433.

Deumlich, D., 2012. Structure and Process - Influence of historical agriculture of linear flow paths by extreme rainfall in Brandenburg. Landscape Online 31, 1-19.

Di Stefano, C., Ferro, V., Porto, P., 2000. Length slope factors for applying the Revised Universal Soil Loss Equation at basin scale in southern Italy. Journal of Agricultural Engineering Research 75, 349-364.

Ehlschlaeger C., 1989. Using the AT search algorithm to develop hydrologic models from digital elevation data. International Geographic Information Systems (IGIS) Symposium '89, 275-281.

Fairfield, J. and Leymarie, P., 1991. Drainage networks from grid digital elevation models. Water Resources Research 27, 709-717

Favis-Mortlock, D., Boardman, J., MacMillan, V., 2001. The limits of erosion modeling: Why We Should Proceed with Care. In: Harmon, R. S., Doe, W. W. (Eds.), Landscape Erosion and Evolution Modeling. Springer, Boston, 477-516.

Fernandez, C., Wu, J. Q., McCool, D. K., Stoeckle, C. O., 2003. Estimating water erosion and sediment yield with GIS, RUSLE, and SEDD. Journal of Soil and Water Conservation 58, 128-136.

Freeman, G.T., 1991. Calculating catchment area with divergent flow based on a regular grid. Computers and Geosciences 17, 413-422.

Fu, G. B., Chen, S. L., McCool, D. K., 2006. Modeling the impacts of no-till practice on soil erosion and sediment yield with RUSLE, SEDD, and ArcView GIS. Soil and Tillage Research 85, 38–49.

Fu, S., Cao, L., Liu, B., Wu, Z., Savabi, M. R., 2015. Effects of DEM grid size on predicting soil loss from small watersheds in China. Environmental Earth Sciences 73, 2141–2151.

Garcia Rodriguez, J. L., Gimenez Suarez, M. C., 2010. Historical review of topographical factor, LS, of water erosion models. Aqua-LAC 2, 56–61.

Garcia Rodriguez, J. L., Gimenez Suarez, M. C., 2012. Methodology for estimating the topographic factor LS of RUSLE3D and USPED using GIS. Geomorphology 175/176, 98–106.

Gertner, G., Wang, G., Fang, S., Anderson, A. B., 2002. Effect and uncertainty of digital elevation model spatial resolutions on predicting the topographical factor for soil loss estimation. Journal of Soil and Water Conservation 57, 164-174.

Hengl, T., 2006. Finding the right pixel size. Computers and Geosciences 32, 1283–1298.

Hickey, R., 2000. Slope angle and slope length solutions for GIS. Cartography 29, 1–8.

Hoffmann, A., da Silva, M. A., Naves Silva, M. L., Curi, N., Klinke, G., de Freitas, D. A. F., 2013. Development of Topographic Factor Modeling for Application in Soil Erosion Models, In: Hernandez Soriano, M. C. (Ed.), Soil Processes and Current Trends in Quality Assessment, pp. 111-138.

Hrabalíková, M. and Janeček, M., 2017. Comparison of different approaches to LS factor calculations based on a measured soil loss under simulated rainfall. Soil and Water Research 12, 69-77.

Hurni, H., 1979. Semien-Äthiopien: Methoden zur Erfassung der Bodenerosion. Geomethodica 4, 151-182.

Ismail, J. and Ravichandran, S., 2008. RUSLE2 model application for soil erosion assessment using remote sensing and GIS. Water Resources Management 22, 83–102.

Kamaludin, H., Lihan, T., Ali Rahman, Z., Mustapha, M. A., Idris, W. M. R., Rahim, S. A., 2013. Integration of remote sensing, RUSLE and GIS to model potential soil loss and sediment yield (SY). Hydrology and Earth System Sciences Discussions 10, 4567–4596.

Keizer, J., Djuma, H., Prasuhn, V., 2016. Soil Erosion by Water. In: Stolte et al. (Eds.), Soil threats in Europe – Status, methods, drivers and effects on ecosystem services. A review report, deliverable 2.1 of the RECARE project. JRC Science and Policy Report, 15-24.

Kienzle, S., 2004. The effect of DEM raster resolution on first order, second order and compound terrain derivatives. Transactions in GIS 8, 83–112.

Koo, J. -Y., Yoon, D. -S., Lee, D. J., Han, J. H., Jung, Y., Yang, J. E., Lim, K. J., 2016. Effect of DEM resolution in USLE LS factor. Journal of Korean Society on Water Environment 32, 89–97.

Kotremba, C., Trapp, M., Thomas, K., 2016. Hochauflösende GIS-basierte Bodenabtragsmodellierungen für ausgewählte Agrarstandorte in Rheinland-Pfalz. Bodenschutz 21, 46-56.

Lane, S. N., Brookes, C. J., Kirkby, M. J., Holden, J., 2004. A network-index-based version of TOPMODEL for use with high-resolution digital topographic data. Hydrological Processes 18, 191–201.

Liu, B. Y., Nearing, M. A., Risse, L. M., 1994. Slope gradient effects on soil loss for steep slopes. Transactions of the ASAE 37, 1835–1840.

Liu, H., Kiesel, J., Hörmann, G., Fohrer, N., 2011. Effects of DEM horizontal resolution and methods on calculating the slope length factor in gently rolling landscapes. Catena 87, 368–375.

Liu, K., Tang, G., Jiang, L., Zhu, A. X., Yang, J., Song, X., 2015. Regional-scale calculation of the LS factor using parallel processing. Computers and Geosciences 78, 110–122.

Maidment, D. R. (Ed.), 2002. Arc hydro: GIS for water resources. 3rd ed. ESRI Press, Redlands, Calif, 203.

Maugnard, A., Bielders, C. L., Bock, L., Colinet, G., Cordonnier, H., Degré, A., Demarcin, D., Dewez, A., Feltz, N., Legrain, X., Pineux, N., Mokadem, A. I., 2013. Cartographie du risqué d'érosion hydrique à l'échelle parcellaire en soutien à la politique agricole wallonne (Belgique). Étude et Gestion des Sols 20, 127-141.

McCool, D. K., Brown, L. C., Foster, G. R., Mutchler, C. K., Meyer, L. D., 1987. Revised slope steepness factor for the Universal Soil Loss Equation. Transactions of the ASAE 30, 1387–1396.

Mitasova, H., Barton, M., Ullah, I., Hofierka, J., Harmon, R. S., 2013. GIS-Based Soil Erosion Modeling. In: Shroder J. F., Bishop, M.P. (Eds.), Treatise on Geomorphology, Elsevier, pp. 228–258.

Mitasova, H., Hofierka, J., Zlocha, M., Iverson, L. R., 1996. Modelling topographic potential for erosion and deposition using GIS. International Journal Geographical Information System 10, 629– 641.

Mondal, A., Khare, D., Kundu, S., Mukherjee, S., Mukhopadhyay, A., Mondal, S., 2017. Uncertainty of soil erosion modelling using open source high resolution and aggregated DEMs. Geoscience Frontiers 8, 425–436.

Moore, I. D. and Burch, G. J., 1986. Physical basis of the Length-Slope Factor in the Universal Soil Loss Equation. Soil Science Society of America Journal 50, 1294-1298.

Moore, I. D. and Wilson, J. P., 1992. Length-slope factors for the revised Universal Soil Loss Equation: simplified method of estimation. Journal of Soil and Water Conservation 47, 423-428.

Moore, I. D., Grayson, R. B., Ladson, A. R., 1991. Digital terrain modelling: A review of hydrological, geomorphological, and biological applications. Hydrological Processes 5, 3–30.

Morgan, R.P.C., 2009. Soil Erosion and Conservation. Blackwell Publishing Ltd., Hoboken.

Naipal, V., Reick, C., Pongratz, J., Van Oost, K., 2015. Improving the global applicability of the RUSLE model - adjustment of the topographical and rainfall erosivity factors. Geoscientific Model Development 8, 2893–2913.

Nearing M. A., 1997. A single, continuous function for slope steepness influence on soil loss. Soil Science Society of America Journal 61, 917–919.

Oliveira, P. T. S., Rodrigues, D. B. B., Sobrinho, T. A., Panachuki, E., Wendland, E., 2013. Use of SRTM data to calculate the (R)USLE topographic factor. Acta Scientiarum. Technology 35, 507-513.

Orlandini, S., Moretti, G., Corticelli, M. A., Santangelo, P. E., Capra, A., Rivola, R., Albertson, J. D., 2012. Evaluation of flow direction methods against field observations of overland flow dispersion. Water Resources Research 48, 13.

Panagos, P., Borrelli P., Poesen J., Ballabio, C., Lugato, E., Meusburger, K., Montanarella, L., Alewell, C., 2015b. The new assessment of soil loss by water erosion in Europe. Environmental Science and Policy 54, 438–447.

Panagos, P., Borrelli, P., Meusburger, K., 2015a. A new European slope length and steepness factor (LS-factor) for modeling soil erosion by water. Geosciences 5, 117–126.

Planchon, O. and Darboux F., 2002. A fast, simple and versatile algorithm to fill the depressions of digital elevation models. Catena 46, 159–176.

Prasuhn, V., 2011. Soil erosion in the Swiss midlands: Results of a 10-year field survey. Geomorphology 126, 32–41.

Prasuhn, V., 2012. On-farm effects of tillage and crops on soil erosion measured over 10 years in Switzerland. Soil and Tillage Research. 120, 137-146.

Prasuhn, V., Liniger, H., Gisler, S., Herweg, K., Candinas, A., Clément, J. -P., 2013. A high-resolution soil erosion risk map of Switzerland as strategic policy support system. Land Use Policy 32, 281–291.

Quinn, P., Beven, K., Chevallier, P., Planchon, O., 1991. The prediction of hillslope flow paths for distributed hydrological modelling using digital terrain models. Hydrological Processes 5, 59-79.

Renard K. G., Foster G. R., Weesies G. A., McCool D. K., Yoder D. C., 1997. Predicting soil erosion by water. A guide to conservation planning with the Revised Universal Soil Loss Equation (RUSLE). Handbook. 703, US Department of Agriculture.

Rymszewicz, A., Mockler, E., O'Sullivan, J., Bruen, M., Turner, J., Conroy, E., Kelly-Quinn, M., Harrington, J., Lawler, D., 2015. Assessing the applicability of the Revised Universal Soil Loss Equation (RUSLE) to Irish Catchments. Proceedings of the International Association of Hydrological Sciences 367, 99–105.

Schäuble, H., 2005. AVErosion 1.1 für ArcView 3.x – Berechnung von Bodenerosion und –akkumulation nach den Modellen USLE und MUSLE87. URL: http://data.terracs.com/pdf/averosion-german.pdf

Seibert, J. and McGlynn, B., 2007. A new triangular multiple flow direction algorithm for computing upslope areas from gridded digital elevation models. Water Resources Research 43, 1-8.

Smith, D. D. and Whitt, D. M., 1947. Estimating Soil Losses from Field Areas of Claypan Soil. Soil Science Society of America Journal 12, 485-490.

Smith, D. D. and Wischmeier, W. H., 1957. Factors affecting sheet and rill erosion. American Geophysical Union Transactions 38, 889-896.

Tarboton, D. G., 1997. A new method for the determination of flow directions and upslope areas in grid digital elevation models. Water Resources Research 33, 309-319.

Tetzlaff, B., Friedrich, K., Vorderbrügge, T., Vereecken, H. , Wendland, F., 2013. Distributed modelling of mean annual soil erosion and sediment delivery rates to surface waters. Catena 102, 13-20.

Thomas, I. A., Jordan, P., Mellander, P. -E., Fenton, O., Shine, O., Ó hUallacháin, D., Creamer, R., McDonald, N. T., Dunlop, P., Murphy, P. N. C., 2016. Improving the identification of hydrologically sensitive areas using LiDAR DEMs for the delineation and mitigation of critical source areas of diffuse pollution. Science of The Total Environment 556, 276–290.

Thomas, I. A., Jordan, P., Shine, O., Fenton, O., Mellander, P. -E., Dunlop, P., Murphy, P. N. C., 2017. Defining optimal DEM resolutions and point densities for modelling hydrologically sensitive areas in agricultural catchments dominated by microtopography. International Journal of Applied Earth Observation and Geoinformation 54, 38–52.

Thompson, J. A., Bell, J. C., Butler, C. A., 2001. Digital elevation model resolution: effects on terrain attribute calculation and quantitative soil-landscape modeling. Geoderma 100, 67–89.

Van Remortel, R. D., Hamilton, M. E., Hickey, R. J., 2001. Estimating the LS factor for RUSLE through iterative slope length processing of digital elevation data. Cartography 30, 27–35.

Volk, M., Möller, M., Wurbs, D., 2010. A pragmatic approach for soil erosion risk assessment within policy hierarchies. Land Use Policy 27, 997–1009.

Wang, L. and Liu, H., 2006. An efficient method for identifying and filling surface depressions in digital elevation models for hydrologic analysis and modelling. International Journal of Geographical Information Science 20, 193–213.

Wang, S., Zhu, X., Zhang, W., Yu, B., Fu, S., Liu, L., 2016. Effect of different topographic data sources on soil loss estimation for a mountainous watershed in Northern China. Environmental Earth Sciences 75, 1382.

Wilson, J. P., Aggett, G., Deng, Y., Lam, C. S., 2008. Water in the landscape: a review of contemporary flow routing algorithms. In: Zhou et al. (Eds.), Advances in Digital Terrain Analysis. Springer, Berlin, 213–236.

Winchell, M. F., Jackson, S. H., Wadley, A. M., Srinivasan, R., 2008. Extension and validation of a geographic information system-based method for calculating the revised universal soil loss equation length-slope factor for erosion risk assessments in large watersheds. Journal of Soil and Water Conservation 63, 105–111.

Wischmeier, W. H. and Smith, D. D., 1978. Predicting Rainfall Erosion Losses – a Guide to Conservation Planning. Handbook No. 537, US Department of Agriculture.

Wu, S., Li, J., Huang, G., 2005. An evaluation of grid size uncertainty in empirical soil loss modeling with digital elevation models. Environmental Modeling and Assessment 10, 33–42.

Yang, X. H., 2015. Digital mapping of RUSLE slope length and steepness factor across New South Wales, Australia. Soil Research 53, 216–225.

Yitayew, M., Pokrzywka, S. J., Renard, K. G., 1999. Using GIS for facilitating erosion estimation. Applied Engineering in Agriculture 15, 295–301.

Zevenbergen, L. W. and Thorne, C. R., 1987. Quantitative analysis of land surface topography. Earth Surface Processes and Landforms 12, 47–56.

Zhang, H., Yang, Q., Li, R., Liu, Q., Moore, D., He, P., Ritsema, C. J., Geissen, V., 2013. Extension of a GIS procedure for calculating the RUSLE equation LS factor. Computers and Geosciences 52, 177–188.

Zhang, H., Yao, Z., Yang, Q., Li, S., Baartman, J. E. M., Gai, L., Yao, M., Yang, X., Ritsema, C. J., Geissen, V., 2017. An integrated algorithm to evaluate flow direction and flow accumulation in flat regions of hydrologically corrected DEMs. Catena 151, 174–181.

Zingg, A. W., 1940. Degree and length of land slope as it affects soil loss in runoff. Agricultural Engineering 21, 59-64.

Highlights

- 21 different L-factor calculations were processed
- Field blocks are crucial for spatial confinement of contributing area
- Various multiple flow algorithms result in similar L-factor values
- DEM2 and DEM25 hardly differ in calculated mean LS-factor values
- DEM2 delivers a very good spatial distribution and reflects reality precise